Inverse regulation of Vibrio cholerae biofilm dispersal by polyamine signals

Andrew A. Bridges^{1,2}, Bonnie L. Bassler^{1,2*}

¹Department of Molecular Biology, Princeton University, Princeton, NJ 08544, USA ²The Howard Hughes Medical Institute, Chevy Chase, MD 20815, USA. *Corresponding author. Email: <u>bbassler@princeton.edu</u>

1 Abstract (148 words)

2 The global pathogen Vibrio cholerae undergoes cycles of biofilm formation and dispersal in the environment and the human host. Little is understood about biofilm dispersal. Here, we show that 3 MbaA, a periplasmic polyamine sensor, and PotD1, a polyamine importer, regulate V. cholerae 4 5 biofilm dispersal. Spermidine, a commonly produced polyamine, drives V. cholerae dispersal, 6 whereas norspermidine, an uncommon polyamine produced by vibrios, inhibits dispersal. 7 Spermidine and norspermidine differ by one methylene group. Both polyamines control dispersal 8 via MbaA detection in the periplasm and subsequent signal relay. Our results suggest that 9 dispersal fails in the absence of PotD1 because endogenously produced norspermidine is not reimported, periplasmic norspermidine accumulates, and it stimulates MbaA signaling. These 10 11 results suggest that V. cholerae uses MbaA to monitor environmental polyamines, blends of which 12 potentially provide information about numbers of 'self' and 'other'. This information is used to dictate whether or not to disperse from biofilms. 13

Main

Introduction

Bacteria frequently colonize environmental habitats and infection sites by forming surfaceattached multicellular communities called biofilms (Flemming et al., 2016). Participating in the biofilm lifestyle allows bacteria to collectively acquire nutrients and resist threats (Flemming et al., 2016). By contrast, the individual free-swimming state allows bacteria to roam. The global pathogen Vibrio cholerae undergoes repeated rounds of clonal biofilm formation and disassembly. and both biofilm formation and biofilm exit are central to disease transmission as V. cholerae alternates between the marine niche and the human host (Conner et al., 2016; Gallego-Hernandez et al., 2020; Tamayo et al., 2010). The V. cholerae biofilm lifecycle occurs in three stages. First, a founder cell attaches to a substate, second, through cycles of growth, division, and extracellular matrix secretion, the biofilm matures, and finally, when the appropriate environmental conditions are detected, cells leave the biofilm through a process termed dispersal (Bridges et al., 2020). Bacterial cells liberated through dispersal can depart their current environment and repeat the lifecycle in a new niche, such as in a new host (Guilhen et al., 2017). In general, the initial stages of the biofilm lifecycle, from attachment through maturation, have been well studied in V. cholerae and other bacterial species, whereas the dispersal phase remains underexplored. Components underlying biofilm dispersal are beginning to be revealed. For example, in many bacterial species, the Lap system that is responsible for cell attachments during biofilm formation is also involved in dispersal (Boyd et al., 2012; Christensen et al., 2020; Gjermansen et al., 2005; Kitts et al., 2019; Newell et al., 2011).

To uncover mechanisms controlling *V. cholerae* biofilm dispersal, we recently developed a brightfield microscopy assay that allows us to follow the entire biofilm lifecycle (Bridges and Bassler, 2019). We combined this assay with mutagenesis and high-content imaging to identify mutants that failed to properly disperse (Bridges et al., 2020). Our screen revealed genes encoding proteins that fall into three functional groups: signal transduction, matrix degradation, and cell motility. Our hypothesis is that these classes of components act in sequence to drive biofilm dispersal. First, the cues that induce dispersal are detected by the signal transduction proteins. Second, activation of matrix digestion components occurs. Finally, cell motility engages and permits cells to swim away from the disassembling biofilm. The majority of the genes identified in the screen encoded signal transduction proteins. Elsewhere, we characterized one of the signaling systems identified in the screen, a new two-component phospho-relay that we named DbfS-DbfR (for Dispersal of Biofilm Sensor and Dispersal of Biofilm Regulator) that controls biofilm dispersal (Bridges et al., 2020). Of the remaining signaling proteins identified in the screen, four are proteins involved in regulating production/degradation of, or responding to, the second messenger molecule cyclic diguanylate (c-di-GMP).

C-di-GMP regulates biofilm formation in many bacteria including *V. cholerae* in which low c-di-GMP levels correlate with motility and high c-di-GMP levels promote surface attachment and matrix production, and thus, biofilm formation (Conner et al., 2017). C-di-GMP is synthesized by enzymes that contain catalytic GGDEF domains that have diguanylate cyclase activity (Conner et al., 2017). C-di-GMP is degraded by proteins with EAL or HD-GYP domains that possess phosphodiesterase activity. *V. cholerae* encodes >50 proteins harboring one or both of these domains, underscoring the global nature of c-di-GMP signaling in this pathogen (Conner et al., 2017). The activities of these enzymes are often regulated by environmental stimuli through ligand binding sensory domains, however, in most cases, the identities of ligands for GGDEF- and EAL-

containing enzymes are unknown (Römling et al., 2013). Of the c-di-GMP regulatory proteins identified in our dispersal screen only one, the hybrid GGDEF/EAL protein, MbaA, which has previously been shown to regulate *V. cholerae* biofilm formation (Bomchil et al., 2003), has a defined environmental stimulus: MbaA responds to the ubiquitous family of small molecules called polyamines, aliphatic cations containing two or more amine groups (Miller-Fleming et al., 2015). Our dispersal screen also identified PotD1, a periplasmic binding protein that mediates polyamine import and that has also been shown to control *V. cholerae* biofilm formation (Cockerell et al., 2014; McGinnis et al., 2009). Thus, identification of these two genes in our screen suggested that beyond roles in biofilm formation, polyamine detection could be central to biofilm dispersal. In the present work, we explore this new possibility.

Polyamines are essential small molecules derived from amino acids and were likely produced by the last universal common ancestor (Michael, 2018; Miller-Fleming et al., 2015). Different organisms make distinct blends of polyamines (Michael, 2018) and they are involved in biological processes ranging from stress responses to signal transduction to protein synthesis to siderophore production (Karatan et al., 2005; McGinnis et al., 2009; Michael, 2018). In some cases, mechanisms underlying polyamine function are known. For example, the eukaryotic translation initiation factor 5A is modified with hypusine that is derived from the polyamine spermidine (Puleston et al., 2019). In most cases, however, the mechanisms by which polyamines control physiology remain mysterious (Miller-Fleming et al., 2015).

Polyamines are known to be involved in biofilm development in many bacterial species (Hobley et al., 2014; Karatan and Michael, 2013; Michael, 2018; Nesse et al., 2015; Patel et al., 2006). Intriguingly, the biofilm alterations that occur in response to a given polyamine vary among species. In V. cholerae, norspermidine, a rare polyamine produced by Vibrionaceae and select other organisms, promotes biofilm formation (Karatan et al., 2005; Lee et al., 2009). In contrast, the nearly ubiquitous polyamine spermidine, which differs from norspermidine only by a single methylene group, is not produced at substantial levels by V. cholerae and it represses V. cholerae biofilm formation (Fig. 1) (Karatan et al., 2005; Lee et al., 2009; McGinnis et al., 2009). Likewise, the polyamine spermine, typically made by eukaryotes, also represses V. cholerae biofilm formation (Sobe et al., 2017). Both spermidine and spermine are abundant in the human intestine (Benamouzig et al., 1997; McEvoy and Hartley, 1975; Osborne and Seidel, 1990). These results have led to the hypothesis that V. cholerae detects norspermidine as a measure of 'self' and spermidine and spermine as measures of 'other' to assess the species composition of the vicinal community (Sobe et al., 2017; Wotanis et al., 2017). V. cholerae funnels that information internally to determine whether or not to make a biofilm (Sobe et al., 2017; Wotanis et al., 2017). V. cholerae produces intracellular norspermidine, however, norspermidine has not been detected in cell-free culture fluids of laboratory grown strains (Parker et al., 2012). Thus, if norspermidine does indeed enable V. cholerae to take a census of 'self', it is apparently not via a canonical quorum-sensing type mechanism.

As mentioned above, information contained in extracellular polyamines is transduced internally by MbaA, which is embedded in the inner membrane. MbaA contains a periplasmic domain that interacts with the periplasmic binding protein NspS. *nspS* is located immediately upstream of *mbaA* in the chromosome (Cockerell et al., 2014; Karatan et al., 2005; Young et al., 2021). MbaA also possesses cytoplasmic GGDEF (SGDEF in MbaA) and EAL (EVL in MbaA) domains (Fig. 1). Genetic evidence suggests that when NspS is bound to norspermidine, the complex associates with MbaA and biofilm formation is promoted (Cockerell et al., 2014).

Specifically, NspS interaction with MbaA inhibits MbaA phosphodiesterase activity, leading to increased c-di-GMP levels, and in turn, elevated biofilm formation (Fig. 1, left panel) (Cockerell et al., 2014). It is proposed that Apo-NspS and NspS bound to spermidine or spermine do not bind to MbaA, and thus, under this condition, biofilm formation is reduced (Cockerell et al., 2014; Sobe et al., 2017). In this case, MbaA phosphodiesterase activity is not inhibited, which leads to decreased c-di-GMP levels and repression of biofilm formation (Fig. 1, right panel). Currently, it is not known whether or not MbaA has diguanylate cyclase activity. The purified MbaA cytoplasmic domain functions as a phosphodiesterase *in vitro* (Cockerell et al., 2014).

In a proposed second regulatory mechanism, norspermidine and spermidine are thought to control biofilm formation via import through the inner membrane ABC transporter, PotABCD1 (McGinnis et al., 2009). Following internalization, via an undefined cytoplasmic mechanism, polyamines are proposed to modulate biofilm formation (Fig. 1) (McGinnis et al., 2009). This hypothesis was based on the finding that elimination of PotD1, which is required for import of norspermidine and spermidine, resulted in elevated biofilm formation. Importantly, the studies reporting the MbaA and PotD1 findings used quorum-sensing deficient *V. cholerae* strains (Joelsson et al., 2006) that likely cannot disperse from biofilms. Furthermore, the end-point biofilm assays used could not differentiate between enhanced biofilm formation and the failure to disperse.

Here, we combine real-time biofilm lifecycle measurements, mutagenesis, a reporter of cytoplasmic c-di-GMP levels, and measurements of intra- and extracellular polyamine concentrations to define the roles that norspermidine and spermidine play in controlling the V. cholerae biofilm lifecycle. In wildtype V. cholerae, exogenous norspermidine and spermidine inversely alter cytoplasmic c-di-GMP levels and they exert their effects through the NspS-MbaA circuit. Norspermidine promotes biofilm formation and suppresses biofilm dispersal. Spermidine represses biofilm formation and promotes biofilm dispersal. Both the MbaA SGDEF and EVL domains are required for polyamine control of the biofilm lifecycle. We provide evidence that MbaA synthesizes c-di-GMP in the presence of norspermidine and degrades c-di-GMP in the presence of spermidine and that is what drives V. cholerae to form and disperse from biofilms, respectively. When MbaA is absent, V. cholerae is unable to alter the biofilm lifecycle in response to extracellular polyamines. We demonstrate that polyamine internalization via PotD1 is not required to promote *V. cholerae* entrance or exit from biofilms, but rather, periplasmic detection of polyamines by MbaA is the key regulatory step. Specifically, our results suggest that the $\Delta potD1$ mutant fails to disperse because it is unable to reimport self-secreted norspermidine. The consequence is that excess periplasmic norspermidine accumulates, is detected by MbaA, and that leads to production of c-di-GMP and suppression of biofilm dispersal. Collectively, our work reveals the mechanisms by which V. cholerae detects and transduces the information contained in polyamine signals into modulation of its biofilm lifecycle. We propose that the polyamine sensing mechanisms revealed in this study allow V. cholerae to distinguish relatives from competitors and potentially the presence of predators in the vicinity and, in response, modify its biofilm lifecycle to appropriately colonize territory or disperse from an existing community.

Figure 1

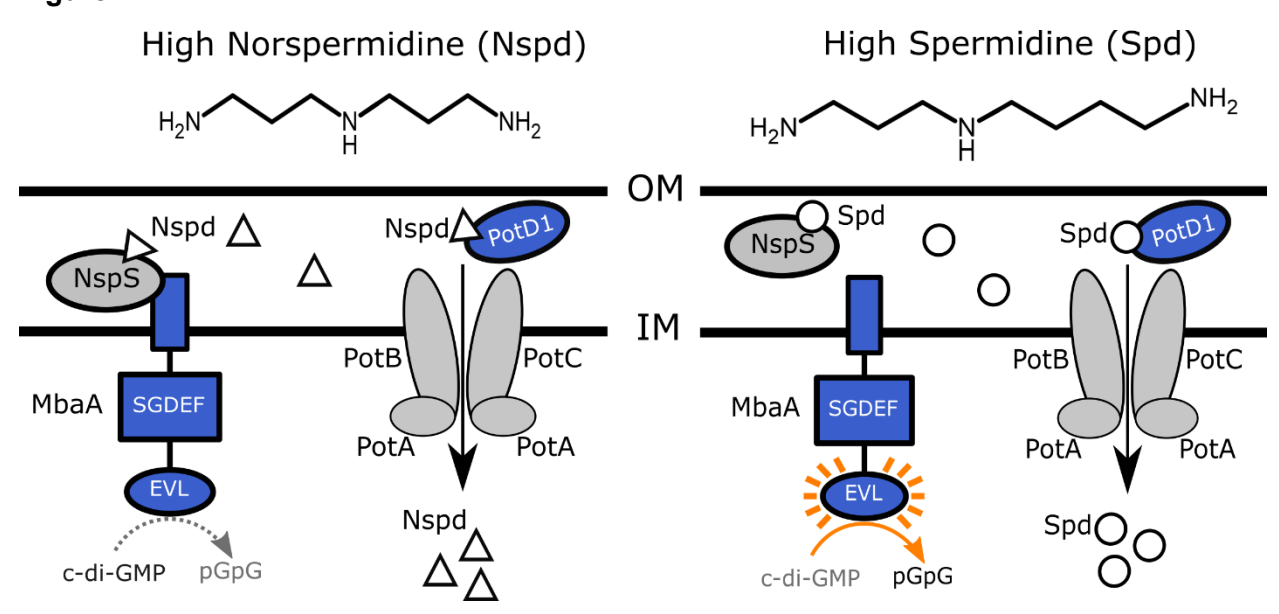


Fig. 1. **Polyamine sensing in** *V. cholerae***.** Schematic showing the previously proposed polyamine detection and import mechanisms in *V. cholerae*. Norspermidine (Nspd, triangles) promotes biofilm formation and spermidine (Spd, circles) represses biofilm formation. The primarily eukaryotic polyamine spermine (not pictured) also signals through the NspS-MbaA pathway. See text for details. OM = outer membrane; IM = inner membrane.

Results

The polyamine signaling proteins MbaA and PotD1 regulate biofilm dispersal by changing c-di-GMP levels

Our combined mutagenesis-imaging screen identified the inner membrane polyamine sensor, MbaA, and the periplasmic polyamine binding protein PotD1 as essential for proper V. cholerae biofilm dispersal motivating us to explore the mechanisms underlying these effects. To probe polyamine signaling across the full biofilm lifecycle, we used our established brightfield imaging assay. In the case of WT V. cholerae, peak biofilm biomass is reached at ~8-9 h of growth, and subsequently, dispersal occurs, and is completed by ~12 h post inoculation (Fig. 2A, B). Deletion of mbaA caused a mild biofilm dispersal defect with no detectable difference in peak biofilm biomass compared to WT, a less than 1 h delay in the onset of dispersal, and 27% biomass remaining at 16 h (Fig. 2A, B). Expression of mbaA from an ectopic locus in the $\Delta mbaA$ mutant complemented the biofilm dispersal defect (Figure 2 - figure supplement 1A). Thus, MbaA is required for WT V. cholerae biofilm dispersal. The $\Delta potD1$ mutant exhibited a 60% greater peak biofilm biomass than WT and nearly all of the biomass remained at 16 h, indicating that PotD1 both represses biofilm formation and promotes biofilm dispersal (Fig. 2A, B). Introduction of potD1 at an ectopic locus in the $\Delta potD1$ mutant drove premature biofilm dispersal and reduced overall biofilm formation (Figure 2 - figure supplement 1B). The differences in severity between the

dispersal phenotypes of the $\Delta mbaA$ and $\Delta potD1$ mutants are noteworthy because these strains behaved similarly in the previous end-point biofilm formation assays (McGinnis et al., 2009).

MbaA has previously been shown to possess phosphodiesterase activity in vitro (Cockerell et al., 2014), thus, we reasoned that MbaA functions by altering cytoplasmic c-di-GMP levels, the consequence of which is changes in expression of genes encoding biofilm components. As far as we are aware, no connection has yet been made between PotD1 and cytoplasmic c-di-GMP levels. To determine if the observed biofilm dispersal defects in the ΔmbaA and ΔpotD1 mutants track with altered c-di-GMP levels, we compared the relative cytoplasmic cdi-GMP levels in the WT, $\Delta mbaA$, and $\Delta potD1$ strains. To do this, we employed a fluorescent reporter construct in which expression of turboRFP is controlled by two c-di-GMP-responsive riboswitches (Zhou et al., 2016). The TurboRFP signal is normalized to constitutively produced amCyan encoded on the same plasmid. Previous studies have demonstrated a linear relationship between reporter output and c-di-GMP levels measured by mass spectrometry (Zhou et al., 2016). Indeed, the reporter showed that deletion of mbaA caused only a moderate increase in cytoplasmic c-di-GMP (8% higher than WT), while the ΔpotD1 mutant produced 39% more signal than WT (Fig. 2C). Thus, MbaA, as expected, mediates changes in c-di-GMP levels, and moreover PotD1-mediated import of polyamines also influences cytoplasmic c-di-GMP concentrations.

In V. cholerae, increased cytoplasmic c-di-GMP levels are associated with elevated extracellular matrix production (called VPS for vibrio polysaccharide) and, in turn, increased biofilm formation. Using a P_{vpsL} -lux promoter fusion that reports on the major matrix biosynthetic operon, we previously showed that matrix gene expression decreases as cells transition from the biofilm to the planktonic state, suggesting that repression of matrix production genes correlates with biofilm dispersal. We wondered how the increased c-di-GMP levels present in the $\Delta mbaA$ and $\Delta potD1$ mutants impinged on vpsL expression. Using the vpsL-lux reporter, we found that the light production patterns mirrored the severities of the dispersal phenotypes and the magnitudes of changes in cytoplasmic c-di-GMP levels: the $\Delta mbaA$ mutant had a light production profile similar to WT, while the $\Delta potD1$ mutant produced 10-fold more light than WT throughout growth. These results indicate that the $\Delta mbaA$ mutant makes normal levels and the $\Delta potD1$ mutant produces excess matrix (Fig. 2D).

As mentioned in the Introduction, our screen revealed three additional genes in c-di-GMP signaling pathways involved in *V. cholerae* biofilm dispersal. While not the focus of the current work, we performed preliminary characterization by deleting these genes and making measurements of their biofilm lifecycle phenotypes, assessing them for changes in cytoplasmic c-di-GMP levels, and quantifying their matrix production profiles (Figure 2 - figure supplement 2 A-D).

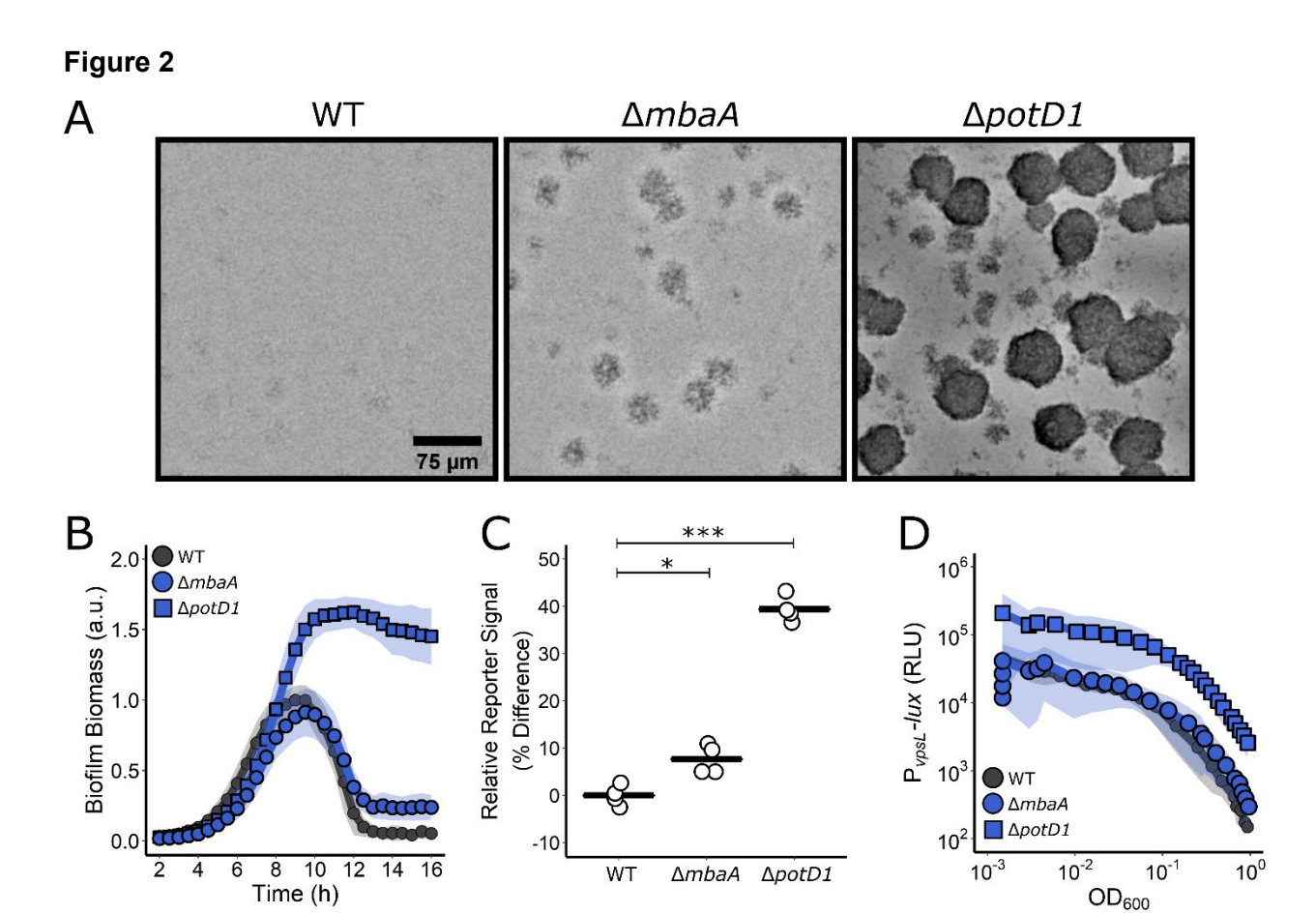


Fig. 2. **Polyamine signaling regulates** *V. cholerae* **biofilm dispersal.** (A) Representative images of the designated *V. cholerae* strains at 16 h. (B) Quantitation of biofilm biomass over time measured by time-lapse microscopy for WT *V. cholerae* and the designated mutants. In all cases, N = 3 biological and N = 3 technical replicates, \pm SD (shaded). a.u., arbitrary unit. (C) Relative c-di-GMP reporter signals for the indicated strains. Values are expressed as the percentage difference relative to the WT strain. N = 4 biological replicates. Each black bar shows the sample mean. Unpaired t-tests were performed for statistical analysis, with P values denoted as *P < 0.05; ***P < 0.001. (D) The corresponding *PvpsL-lux* outputs for the strains and growth conditions as in C. For *vpsL-lux* measurements, N = 3 biological replicates, \pm SD (shaded). RLU, relative light units.

Norspermidine and spermidine inversely regulate *V. cholerae* biofilm dispersal

Above, we show that polyamine signaling proteins are required for normal *V. cholerae* biofilm dispersal. Previous studies demonstrated that norspermidine and spermidine have opposing effects on biofilm formation in end-point assays (Karatan et al., 2005; McGinnis et al., 2009). We wondered if and how these two polyamines affect each stage of the biofilm lifecycle – biofilm formation *and* biofilm dispersal. To investigate their roles, we assayed the biofilm lifecycle in WT *V. cholerae* and our mutants following exogenous administration of norspermidine and spermidine, alone and in combination. Addition of 100 μM norspermidine strongly promoted biofilm formation and completely prevented biofilm dispersal while 100 μM spermidine dramatically reduced biofilm formation and promoted premature biofilm dispersal (Fig. 3A, Video 1). *vpsL-lux* expression increased by > 10-fold following norspermidine treatment and decreased >10-fold following spermidine treatment (Fig. 3B). These results show that norspermidine and spermidine have opposing activities with regard to biofilm formation and dispersal: norspermidine drives biofilm formation by inducing matrix production and this prevents biofilm dispersal and spermidine, by suppressing matrix production prevents biofilm formation and drives biofilm dispersal.

We wondered by what mechanism the information encoded in exogenous polyamines was translated into alterations in matrix gene expression and subsequent changes in biofilm dispersal. We reasoned that MbaA and/or PotD1-mediated changes in cytoplasmic c-di-GMP levels could be responsible. To test this possibility, we assessed how changes in cytoplasmic c-di-GMP levels tracked with changes in extracellular polyamine levels by measuring the c-di-GMP reporter output in response to supplied mixtures of norspermidine and spermidine (Fig. 3C). In the heatmaps, teal and purple represent the lowest and highest values of reporter output, respectively. When provided alone and above a concentration of 10 µM, norspermidine and spermidine strongly increased and decreased, respectively, c-di-GMP reporter activity. At the limit, relative to the WT, norspermidine increased the c-di-GMP reporter output by ~60% while spermidine reduced reporter output by ~25%. Notably, consistent with previous end-point biofilm assays, when norspermidine was present above 50 µM, it overrode the effect of exogenous addition of spermidine, irrespective of spermidine concentration (Fig. 3C) (McGinnis et al., 2009). Thus, V. cholerae cytoplasmic c-di-GMP levels are responsive to extracellular blends of polyamines. When norspermidine is abundant, V. cholerae produces high levels of c-di-GMP, matrix expression is increased, and biofilms do not disperse. In contrast, when spermidine is abundant and norspermidine is absent or present below a threshold concentration, V. cholerae c-di-GMP levels drop, matrix production is repressed, and biofilm dispersal occurs.

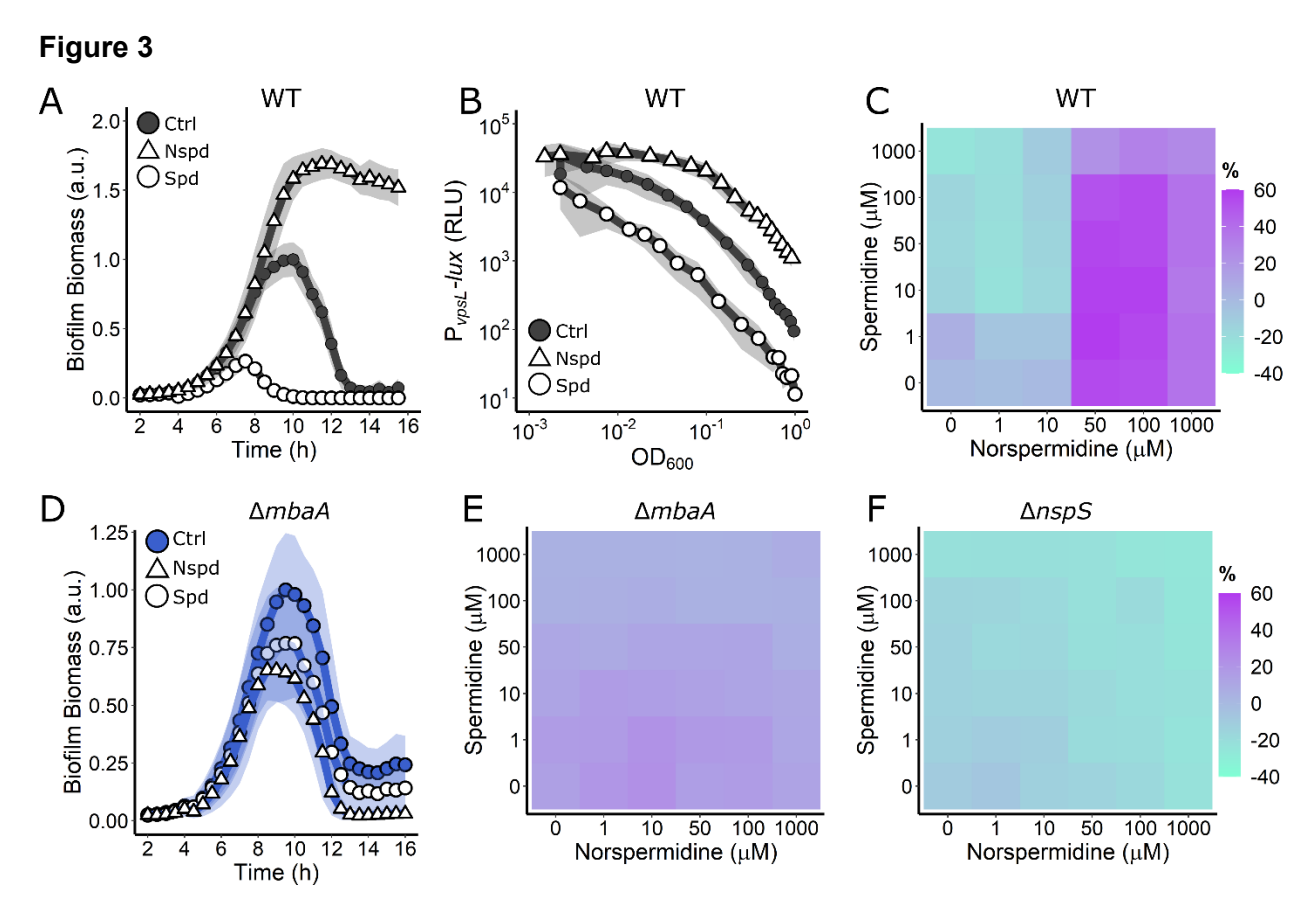


Fig. 3. **Periplasmic detection of polyamines controls** *V. cholerae* **biofilm dispersal.** (A) Quantitation of biofilm biomass over time measured by time-lapse microscopy following addition of water (Ctrl), 100 μ M norspermidine, or 100 μ M spermidine to WT *V. cholerae*. (B) Light output from the *PvpsL-lux* reporter for the treatments in A over the growth curve. (C) C-di-GMP reporter output at the indicated polyamine concentrations for WT *V. cholerae*. Relative reporter signal (% difference) is displayed as a heatmap (teal and purple represent the lowest and highest reporter output, respectively). (D) As in A for the Δ mbaA mutant. (E) As in C for the Δ mbaA mutant. (F) As in C for the Δ nspS mutant. Biofilm biomass data are represented as means normalized to the peak biofilm biomass of the Ctrl condition. In all biofilm biomass measurements, *N* = 3 biological and *N* = 3 technical replicates, \pm SD (shaded). a.u., arbitrary unit. In *vpsL-lux* measurements, *N* = 3 biological replicates, \pm SD (shaded). RLU, relative light units. For the c-di-GMP reporter assays, values are expressed as the percentage difference relative to the untreated WT strain, allowing comparisons to be made across all heatmaps in all figures in this manuscript. The same color bar applies to all heatmaps in this manuscript. For each condition, *N* = 3 biological replicates. Numerical values and associated SDs are available in Supplementary File 1.

MbaA transduces external polyamine information internally to control biofilm dispersal

Our data show that both the MbaA periplasmic polyamine sensor and the PotD1 polyamine importer are required for biofilm dispersal. Our next goal was to distinguish the contribution of periplasmic detection from cytoplasmic import of polyamines to the biofilm lifecycle. We began with periplasmic polyamine detection, mediated by NspS together with MbaA. We supplied

norspermidine or spermidine to the $\triangle mbaA$ mutant and monitored biofilm biomass over time. To our surprise, the $\Delta mbaA$ mutant was impervious to the addition of either polyamine as both polyamines caused only a very modest reduction in overall biofilm biomass, and dispersal timing resembled the untreated ΔmbaA control (Fig. 3D, Video 1). Consistent with this result, titration of the polyamines alone and in combination onto the ΔmbaA strain carrying the c-di-GMP reporter did not substantially alter reporter output (Fig. 3E). These results show that the dynamic response of WT to polyamines requires MbaA. We suspect that the minor reduction in biofilm production that occurred in the $\Delta mbaA$ mutant when supplied polyamines is due to non-specific effects, perhaps via interaction of polyamines with negatively charged matrix components. We next investigated the role of the polyamine periplasmic binding protein NspS that transmits polyamine information to MbaA. In the absence of its partner polyamine binding protein, NspS, MbaA is thought to function as a constitutive phosphodiesterase (Cockerell et al., 2014). Consistent with this model, deletion of nspS in an otherwise WT strain reduced overall peak biofilm biomass by 65% and dispersal initiated 4 h prior to when dispersal begins in the WT (Figure 3 - figure supplement 1). In the $\triangle nspS$ mutant, c-di-GMP levels were lower than in the WT as judged by the c-di-GMP reporter (Fig. 3F) showing that MbaA is locked as a constitutive phosphodiesterase. Exogenous addition of polyamines had no effect on c-di-GMP levels (Fig. 3F). Together, these findings demonstrate that the WT V. cholerae response to polyamines is controlled by the NspS-MbaA polyamine sensing circuit.

237

238

239

240

241

242

243

244

245

246

247

248

249

250

251

252

253

254255

256

257

258

259

260

261

262

263

264

265266

267

268

269270

271

272

273

274275

276

277278

279

280

Both the MbaA EVL and SGDEF domains are required for MbaA to detect polyamines

We wondered how the putative MbaA phosphodiesterase and diguanylate cyclase enzymatic activities contribute to the *V. cholerae* responses to norspermidine and spermidine. The cytoplasmic domain of MbaA exhibits phosphodiesterase but not diguanylate cyclase activity in vitro (Cockerell et al., 2014). We reasoned that, when an intact regulatory domain is present, MbaA could possess both enzymatic activities, with the activity of each domain inversely controlled by NspS binding. To probe the role of each domain, we introduced inactivating point mutations in the catalytic motifs. To ensure that our mutations did not destabilize MbaA, we first fused MbaA to 3xFLAG and introduced the gene encoding the fusion onto the chromosome at the mbaA locus. Tagging did not alter MbaA control over the biofilm lifecycle (Figure 4 - figure supplement 1A, Video 2). To inactivate the MbaA phosphodiesterase activity, we substituted the conserved catalytic residue E553 with alanine, converting EVL to AVL (referred to as EVL* henceforth). This change did not alter MbaA-3xFLAG abundance (Figure 4 - figure supplement 1B). V. cholerae harboring MbaA^{EVL*} exhibited an increase in biofilm biomass and a strong biofilm dispersal defect (Fig. 4A), and only a modest response to exogenous polyamines, with norspermidine eliciting some inhibition of biofilm dispersal and spermidine driving a small reduction in overall biofilm biomass (Fig. 4B, Video 2). Treatment with norspermidine did increase c-di-GMP levels in *V. cholerae* carrying MbaA^{EVL*} as judged by the reporter output (Fig. 4C), albeit not to the level of WT (Fig. 3C), suggesting that the V. cholerae mbaA^{EVL*} mutant, which is incapable of c-di-GMP degradation, retains the capacity to synthesize some c-di-GMP via the MbaA SGDEF domain. In contrast, the *V. cholerae mbaA^{EVL*}* strain displayed little reduction in cdi-GMP levels in response to spermidine, presumably because it lacks the phosphodiesterase activity required to degrade c-di-GMP (Fig. 4C). Thus, despite the fact that the purified cytoplasmic domain functioned only as a phosphodiesterase in vitro, our results suggest that, in vivo, MbaA is capable of synthesizing c-di-GMP in the presence of norspermidine. To validate

this prediction, we altered the conserved catalytic residues D426 and E427 to alanine residues, yielding the inactive MbaA SGAAF variant (referred to as SGDEF*). These substitutions did not affect protein levels (Figure 4 - figure supplement 1B). In every regard, the *mbaA*^{SGDEF*} mutant behaved identically to the Δ*mbaA* mutant. The *V. cholerae mbaA*^{SGDEF*} mutant exhibited a modest biofilm dispersal defect (Fig. 4A) and biofilm biomass was reduced in response to exogenous norspermidine and spermidine (Fig. 4D, Video 2). Furthermore, addition of polyamines to the *mbaA*^{SGDEF*} mutant harboring the c-di-GMP reporter did not drive substantial changes in reporter output (Fig. 4E). These results show that the MbaA SGDEF domain is indispensable for the MbaA response to polyamines.

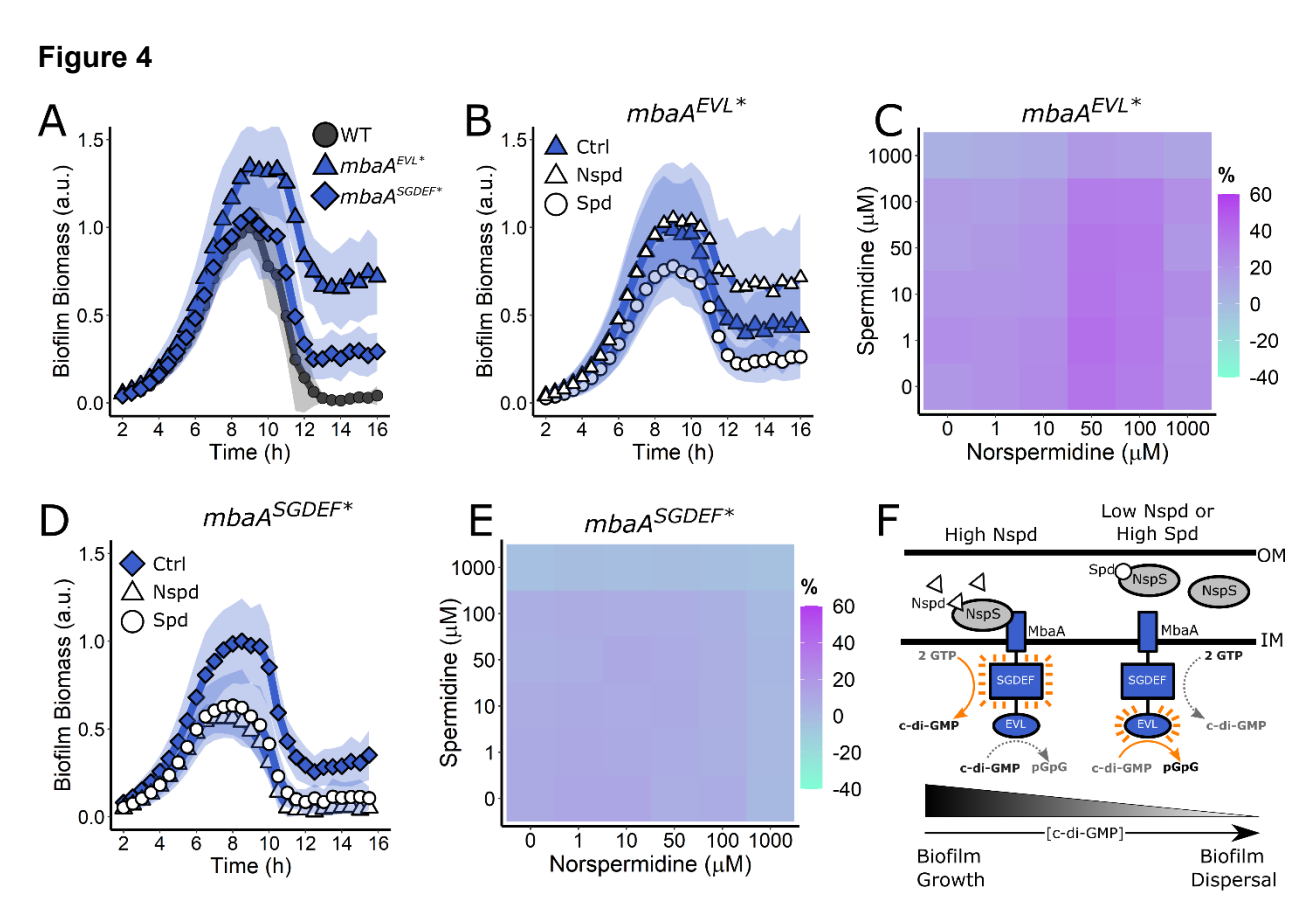


Fig. 4. Both the MbaA SGDEF and EVL domains are required for regulation of *V. cholerae* biofilm dispersal. (A) Quantitation of biofilm biomass over time for the *V. cholerae* strains carrying mbaA-3xFLAG, $mbaA^{EVL^*}$ -3xFLAG, and $mbaA^{SGDEF^*}$ -3xFLAG. (B) Quantitation of biofilm biomass over time measured by time-lapse microscopy for *V. cholerae* carrying $mbaA^{EVL^*}$ -3xFLAG following addition of a water (Ctrl), 100 µM norspermidine, or 100 µM spermidine. (C) C-di-GMP reporter output at the indicated polyamine concentrations for *V. cholerae* carrying $mbaA^{EVL^*}$ -3xFLAG. Relative reporter signal (% difference) is displayed as a heatmap (teal and purple represent the lowest and highest reporter output, respectively). (D) As in B for the $mbaA^{SGDEF^*}$ -3xFLAG mutant. (E) As in C for the $mbaA^{SGDEF^*}$ -3xFLAG mutant. (F) Schematic representing the proposed MbaA activities in response to norspermidine and spermidine. Biofilm biomass data are represented as means normalized to the peak biofilm biomass of the WT strain or Ctrl condition. In all cases, N = 3 biological and N = 3 technical replicates, \pm SD (shaded). a.u.,

arbitrary unit. In the c-di-GMP reporter assays, values are expressed as the percentage difference relative to the untreated WT strain, allowing comparisons to be made across all heatmaps in all figures in this manuscript. The same color bar applies to all panels in this manuscript. For each condition, N = 3 biological replicates. Numerical values and associated SDs are available in Supplementary File 1. In panel F, OM = outer membrane; IM = inner membrane.

Based on the results in Figs. 3 and 4, we conclude that the MbaA phosphodiesterase and diguanylate cyclase domains are both required for MbaA to respond properly to polyamines to regulate *V. cholerae* biofilm dispersal. We propose a model in which, elevated periplasmic norspermidine levels drive NspS to bind to MbaA. Consequently, MbaA phosphodiesterase activity is suppressed and the diguanylate cyclase activity dominates, which leads to c-di-GMP accumulation and commitment to the biofilm lifestyle (Fig. 4F). In contrast, when spermidine is detected, or when periplasmic polyamine concentrations are low, NspS dissociates from MbaA. Consequently, MbaA diguanylate cyclase activity is suppressed and its phosphodiesterase activity dominates, which leads to a reduction in cytoplasmic c-di-GMP and favors biofilm dispersal (Fig. 4F).

290

291

292

293

294

295

296

297

298

299

300

301

302

303

304

305

306

307

308

309

310

311

312

313

314

315

316

317

318

319 320

321

322

323

324

325

326

Polyamines control the V. cholerae biofilm lifecycle via periplasmic detection, not via import into the cytoplasm

Here, we investigate the role of PotD1 in controlling biofilm dispersal. Addition of norspermidine did not alter the non-dispersing phenotype of the $\Delta potD1$ mutant, whereas spermidine treatment drove premature biofilm dispersal and a reduction in peak biofilm biomass (Fig. 5A, Video 1). Consistent with these findings, addition of norspermidine to the \(\Delta potD1 \) strain did not alter the cdi-GMP reporter output, whereas addition of spermidine reduced output signal, but only at the highest concentrations tested (Fig. 5B). These biofilm lifecycle and reporter results show that PotD1-mediated import is not required for spermidine to modulate the biofilm lifecycle. Thus, we considered an alternative mechanism to underlie the V. cholerae ΔpotD1 phenotype. We hypothesized that endogenously produced norspermidine is secreted into the periplasm. In the case of WT V. cholerae, the equilibrium between norspermidine release and PotD1-mediated reuptake places MbaA into a partially liganded state, and as a consequence, MbaA exhibits modest net phosphodiesterase activity (Fig. 5C). In the V. cholerae ΔpotD1 mutant that cannot reimport norspermidine, we predict that periplasmic norspermidine levels become elevated, NspS detects norspermidine, binds to MbaA, and promotes the MbaA diguanylate cyclase active state (Fig. 5D). Hence, c-di-GMP is synthesized and biofilm dispersal is prevented. This hypothesis is consistent with our result showing that addition of norspermidine to the ΔpotD1 mutant does not cause any change in biofilm dispersal. Presumably, in the ΔpotD1 mutant, the NspS protein is already saturated due to elevated periplasmic levels of endogenously produced norspermidine. If this hypothesis is correct, norspermidine biosynthesis would be a requirement for biofilm formation because in the absence of norspermidine production, NspS would remain unliganded, and MbaA would function as a constitutive phosphodiesterase (Fig. 5E). Indeed, and consistent with previous results, the $\triangle nspC$ mutant that lacks the carboxynorspermidine decarboxylase enzyme NspC that is required for norspermidine synthesis, failed to form biofilms (Fig. 5F and Lee et al., 2009; McGinnis et al., 2009). Furthermore, the ΔnspC ΔpotD1 double mutant also failed to form biofilms, showing that endogenous norspermidine biosynthesis is required for the $\Delta potD1$

mutation to exert its effect (Fig. 5F). Consistent with these interpretations, the $\Delta mbaA$ mutation is epistatic to the $\Delta potD1$ mutation as the $\Delta mbaA$ $\Delta potD1$ double mutant exhibited a dispersal phenotype indistinguishable from the single $\Delta mbaA$ mutant (Fig. 5G). Administration of exogenous norspermidine or spermidine to the $\Delta mbaA$ $\Delta potD1$ double mutant (Fig. 5H, Video 1) mimicked what occurred following addition to the single $\Delta mbaA$ mutant (Fig. 3D): that is, essentially no response. Thus, information from externally supplied polyamines is transduced internally by MbaA and not via PotD1-mediated import. Lastly, to confirm that the observed $\Delta potD1$ phenotype was due to a defect in norspermidine transport, rather than a defect in periplasmic binding and sequestration of norspermidine, we deleted potA, encoding the ATPase that supplies the energy required for polyamine import through the PotABCD1 transporter (Kashiwagi et al., 2002). In the absence of PotA, PotD1 remains capable of binding polyamines, but no transport occurs. The $\Delta potA$ mutant exhibited the identical dispersal defect as the $\Delta potD1$ mutant demonstrating that transport of norspermidine, not sequestration by PotD1, is the key activity required for WT V. cholerae biofilm dispersal (Figure 5 - figure supplement 1).

To investigate the supposition that the $\Delta potD1$ strain possesses higher levels of periplasmic norspermidine than WT *V. cholerae*, one needs to isolate and measure polyamines in the periplasmic compartment. Unfortunately, we were unable to reliably obtain periplasmic compartment material. We reasoned, however, that some periplasmic norspermidine would diffuse into the extracellular environment, where it could be isolated and quantified, providing us a means to evaluate differences in periplasmic norspermidine levels between the WT and the ΔpotD1 mutant. At high cell density, approximately 25-fold more norspermidine was present in cell-free culture fluids collected from the ΔpotD1 mutant (average 2.3 μM) than in those prepared from the WT (average 90 nM) (Fig. 5I). Norspermidine was nearly undetectable in culture fluids from the $\Delta nspC$ mutant (Fig. 5I). There was no difference in norspermidine levels in whole cell extracts prepared from WT (average 0.6 μmol/g) and the ΔpotD1 mutant (average 0.5 μmol/g) (Fig 5J). Thus, the difference we measured in norspermidine concentrations in the two extracellular fractions cannot be due to variations in norspermidine biosynthesis between the two strains. As expected, both the cell-free fluid and the whole-cell extract from the $\Delta nspC$ mutant were devoid of norspermidine and spermidine (Fig. 5J and Fig. 5 - figure supplement 2), and consistent with previous reports (Lee et al., 2009), only trace spermidine could be detected in the WT intra- and extracellular preparations (Fig. 5 – figure supplement 2). For reference, we also measured the intra- and extracellular levels of cadaverine and putrescine from the same samples (Fig. 5 - figure supplement 2). Thus, our results argue against a cytoplasmic role for norspermidine in the biofilm lifecycle. Rather, our results indicate that the non-dispersing phenotype of the ΔpotD1 strain is due to elevated accumulation of periplasmic norspermidine stemming from the failure of the mutant to reuptake self-made norspermidine. The consequence is that, compared to WT *V. cholerae*, in the Δ*potD1* mutant, MbaA is biased in favor of c-di-GMP production and commitment to the biofilm lifestyle (Fig. 5D).

Figure 5

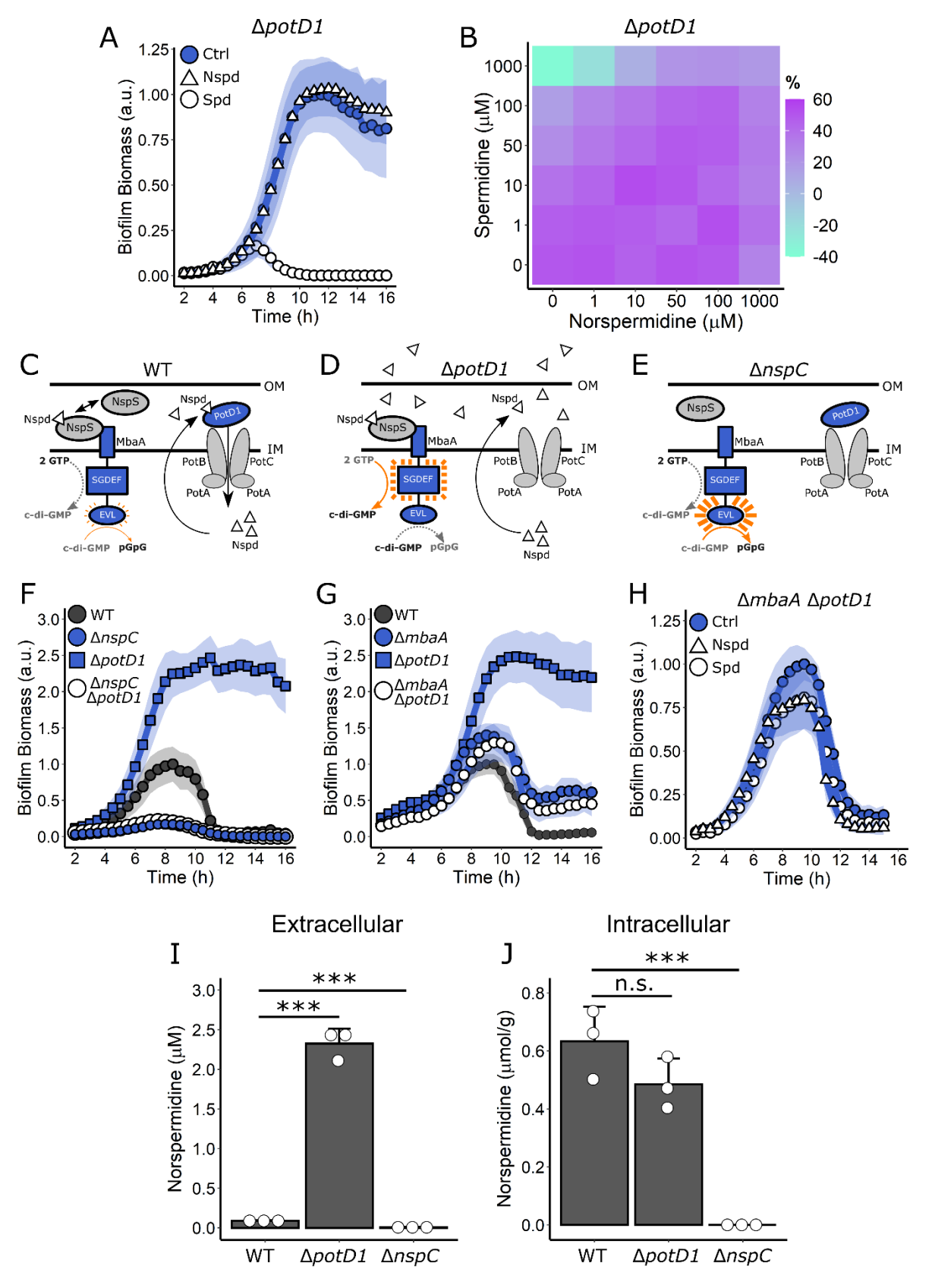


Fig. 5. Polyamine import is not required for MbaA regulation of V. cholerae biofilm dispersal but is required to reduce external norspermidine levels. (A) Quantitation of biofilm biomass over time measured by time-lapse microscopy following addition of water (Ctrl), 100 µM norspermidine, or 100 μM spermidine to the Δ*potD1* mutant. (B) C-di-GMP reporter output at the indicated polyamine concentrations for the ΔpotD1 strain. Relative reporter signal (% difference) is displayed as a heatmap (teal and purple represent the lowest and highest reporter output, respectively). Values are expressed as the percentage difference relative to the untreated WT strain, allowing comparisons to be made across all heatmaps in all figures in the manuscript. The same color bar applies to all c-di-GMP reporter heatmaps in the manuscript and for each condition, N = 3 biological replicates. Numerical values and associated SDs are available in Supplementary File 1. (C) Schematic of NspS-MbaA periplasmic detection of polyamines and polyamine import by PotD1 in WT *V. cholerae*. OM = outer membrane; IM = inner membrane. (D) Schematic of NspS-MbaA periplasmic detection of norspermidine together with the accumulation of elevated extracellular norspermidine in the V. cholerae ΔpotD1 mutant. (E) Schematic of NspS-MbaA activity in the $\triangle nspC$ mutant that is incapable of norspermidine biosynthesis. (F) Biofilm biomass over time for WT, the $\triangle nspC$ mutant, the $\triangle potD1$ mutant, and the $\triangle nspC$ $\triangle potD1$ double mutant. (G) As in F for WT, the $\Delta mbaA$ mutant, the $\Delta potD1$ mutant, and the $\Delta mbaA$ $\Delta potD1$ double mutant. (H) As in A for the $\Delta mbaA$ $\Delta potD1$ double mutant. All biofilm biomass data are represented as means normalized to the peak biofilm biomass of the WT strain or Ctrl condition and in all cases, N = 3 biological and N = 3 technical replicates, \pm SD (shaded). a.u., arbitrary unit. (I) Concentration of norspermidine in cell-free culture fluids for the WT, $\Delta potD1$, and $\Delta nspC$ strains grown to $OD_{600} = 2.0$, measured by mass spectrometry. (J) Intracellular norspermidine levels normalized to wet cell pellet mass for the strains in I. The strains used in panels I and J also contained a ΔvpsL mutation to abolish biofilm formation. Thus, all strains existed in the same growth state which enabled comparisons between strains and, moreover, eliminated any possibility of polyamine sequestration by the biofilm matrix. For I and J, N = 3 biological replicates. error bars represent standard deviation and unpaired t tests were performed for statistical analysis. n.s.= not significant; ***P < 0.001.

MbaA and polyamine levels remain constant throughout the V. cholerae biofilm lifecycle

365

366

367

368

369

370

371

372

373

374

375

376

377

378 379

380

381

Our results demonstrate that WT *V. cholerae* is poised to respond to exogenous polyamines through the NspS-MbaA signaling circuit, presumably allowing *V. cholerae* to adapt to the species composition of its environment. We wondered if, under the conditions of our biofilm assay, MbaA receptor abundance or endogenously produced norspermidine/spermidine levels change over the course of the biofilm lifecycle, either or both of which could influence the normal biofilm growth to dispersal transition. To test these possibilities, we measured MbaA-3xFLAG protein levels and the concentrations of intra- and extracellular polyamines during biofilm formation (T= 5 h) and after dispersal (T = 10 h) in WT *V. cholerae*. MbaA abundance and the intracellular concentrations of norspermidine and spermidine did not fluctuate between the 5 h and 10 h timepoints (Fig. 6A, B). The concentration of extracellular norspermidine did increase between 5 h and 10 h, from <10 nM to ~75 nM (Fig. 6B), however this range is far below the NspS-MbaA detection threshold (Fig. 3C). Extracellular spermidine was nearly undetectable at both timepoints (Fig. 6B). Measurements of additional polyamines from the same samples are shown in Fig. 6 – figure supplement 1. We take these results to mean that, in the absence of exogenously-supplied polyamines, MbaA activity is constant and, in our experiments, the enzyme



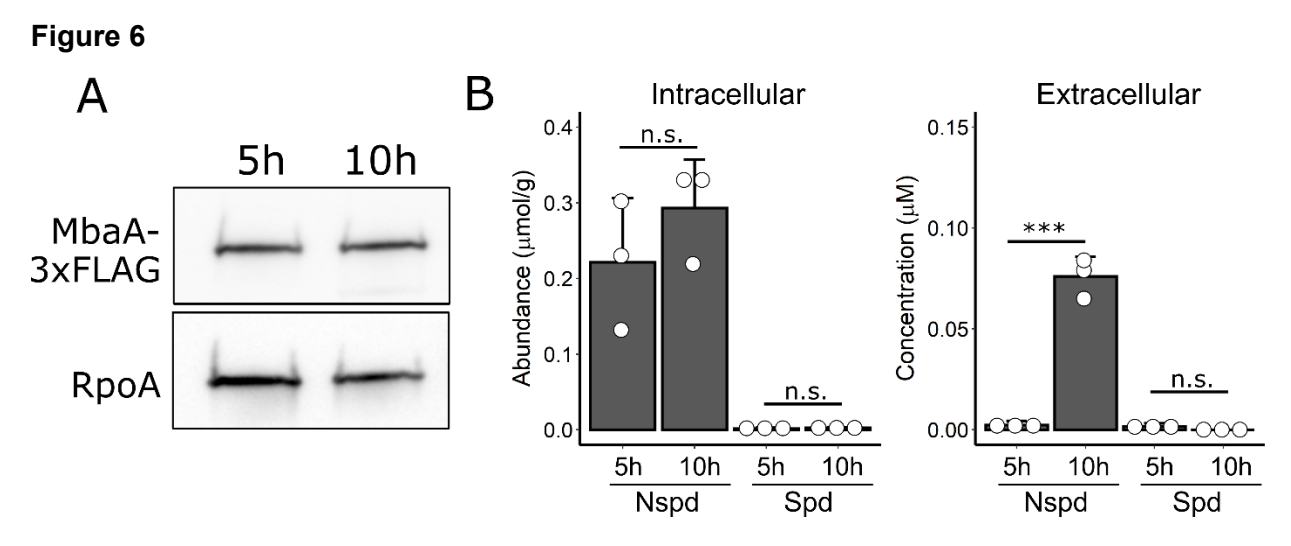


Fig. 6. **MbaA** and intracellular polyamine levels remain constant throughout the biofilm lifecycle. (A) Top panel: Western blot showing MbaA-3xFLAG levels at 5 h and 10 h post inoculation. Bottom panel: The RpoA loading control. Data are representative of three biological replicates. (B) Measurements of intracellular (left panel) and extracellular (right panel) norspermidine (Nspd) and spermidine (Spd) levels at 5 h and 10 h post inoculation. Intracellular levels were normalized to wet cell pellet mass. N = 3 biological replicates, error bars represent SDs and unpaired t tests were performed for statistical analysis. n.s.= not significant; ***P < 0.001.

Discussion

384

385

386

387

388

389

390

391

392

393

394

395

396

397

398

399

400

401

402

In this study, we investigated the effects of the polyamines norspermidine and spermidine on V. cholerae biofilm dispersal. Norspermidine and spermidine, which differ in structure only by one methylene group, mediate starkly opposing effects on the V. cholerae biofilm lifecycle: norspermidine inhibits and spermidine promotes biofilm dispersal. Both function through the NspS-MbaA circuit. Thus, the polyamine binding protein NspS must harbor the exquisite capability to assess the presence or absence of a single chemical moiety, as norspermidine binding drives NspS interaction with MbaA whereas binding to spermidine prevents this interaction. Here, we speculate on the possible biological significance of our findings. We suspect that norspermidine and spermidine act as 'self' and 'other' cues, respectively. Specifically, norspermidine is a rare polyamine in the biosphere, produced only by select organisms, namely *V. cholerae* and closely related marine vibrios (Hamana, 1997; Michael, 2018; Yamamoto et al., 1991). The observation that laboratory grown WT V. cholerae releases little norspermidine, at least in part due to PotD1mediated reuptake (Fig. 5C), suggests that this system does not behave like a canonical quorum sensing pathway. However, it is possible that norspermidine is secreted by *V. cholerae* under some environmental conditions, or by other vibrios, and V. cholerae detects the released norspermidine via NspS-MbaA, and its dispersal from biofilms is prevented. Thus, when close relatives are nearby, as judged by detection of the presence of norspermidine, V. cholerae elects to remain in its current biofilm niche. More speculative is the notion that norspermidine functions

as a cue for phage-, predator-, or toxin-induced cell lysis. Specifically, if *V. cholerae* can detect norspermidine released by neighboring lysed *V. cholerae* cells, in response to the perceived danger, *V. cholerae* would remain in the protective biofilm state. Conversely, detection of spermidine, a nearly ubiquitously produced polyamine (Michael, 2018), could alert *V. cholerae* to the presence of competing or unrelated organisms. In this case, *V. cholerae* would respond by dispersing from biofilms and fleeing that locale. In a seemingly parallel scenario, we previously discovered that autoinducer Al-2, a universally produced quorum-sensing signal, also drove *V. cholerae* biofilm repression and premature dispersal, while CAl-1, the *V. cholerae* 'kin' quorum-sensing autoinducer did not (Bridges and Bassler, 2019). Together, our findings suggest that *V. cholerae* possesses two mechanisms to monitor its own numbers (norspermidine and CAl-1) and two mechanisms to take a census of unrelated organisms in the environment (spermidine and Al-2), and it responds by remaining in the biofilm state when closely related species are in the majority and by exiting the biofilm state when the density of non-related organisms is high, presumably to escape competition/danger.

We found that periplasmic polyamine detection by NspS-MbaA, but not polyamine import, controls the biofilm dispersal program and both the MbaA EVL and SGDEF domains are required for the *V. cholerae* response to polyamines. Despite previous work suggesting that MbaA functions exclusively as a phosphodiesterase and that its SGDEF domain, which possesses a serine substitution in the active site relative to the canonical GGDEF active site, is inert with respect to c-di-GMP synthesis, our data suggest that when norspermidine is present, MbaA does synthesize c-di-GMP (Fig. 3C, Fig. 4C), as has also been shown for other SGDEF proteins (Pérez-Mendoza et al., 2011). Therefore, MbaA is likely a bifunctional protein capable of both c-di-GMP synthesis and degradation. We wonder how such an arrangement benefits *V. cholerae* in its response to polyamines. We speculate that the ability of MbaA to inversely alter c-di-GMP levels in response to two discrete cues coordinates polyamine signaling and enables more rapid and greater magnitude changes in c-di-GMP levels than would be achievable if two separate receptors existed, each harboring only a single catalytic activity and each responsive to only one polyamine.

An analogous bifunctional arrangement exists for the quorum-sensing two-component receptor LuxN from *Vibrio harveyi*. LuxN is an inner membrane receptor that harbors a periplasmic sensory domain responsible for detection of a self-made small molecule cue, a homoserine lactone agonist with a four-carbon acyl tail (Bassler et al., 1994). The ligand encodes species-specific information about cell population density. Competing bacterial species that co-occupy the niche in which *V. harveyi* resides produce similar acyl homoserine lactone signal molecules, and notably, those molecules differ only in the acyl tail length or decoration (Papenfort and Bassler, 2016). The tails of the molecules produced by the competitors usually possess more than four carbons and they act as potent LuxN antagonists. With respect to mechanism, the self-made agonist drives LuxN into phosphatase-mode while the antagonists induce LuxN to act as a kinase (Ke et al., 2015). Thus, as in the MbaA circuit, binding of the different ligands to LuxN propels opposing enzymatic activities in the cytoplasm. We speculate that ligand-driven alternation between opposing enzymatic activities could be an underappreciated mechanism that sensors employ to transmit species-specific and species-non-specific information into discrete changes in downstream behaviors.

In addition to conveying information about the species composition of the vicinal community, the MbaA SGDEF and EVL domains could also participate in dimerization and/or allosteric binding to c-di-GMP or other metabolites to mediate feedback regulation of the opposing

MbaA activities. Parallel examples exist, here we present one: *Caulobacter crescentus* contains a GGDEF/EAL protein called CC3396, in which the GGDEF domain is non-catalytic but it nonetheless binds to GTP, which allosterically activates the phosphodiesterase activity in the neighboring EAL domain (Christen et al., 2005). A feedback mechanism could provide MbaA with the ability to integrate the information encoded in extracellular polyamine blends with cytoplasmic cues, such as the metabolic state of the cell or the current cytoplasmic c-di-GMP level. Taken together, the double ligand detection capability linked to the dual catalytic activities of the NspS-MbaA circuit allows *V. cholerae* to distinguish between remarkably similar ligands and, in response, have the versatility to convey distinct information into the cell to alter the biofilm lifecycle.

In summary, four signaling pathways have now been defined that feed into the regulation of *V. cholerae* biofilm dispersal: starvation (RpoS) (Singh et al., 2017), quorum sensing (via CAI-1 and AI-2) (Bridges and Bassler, 2019; Singh et al., 2017), the recently identified DbfS/DbfR cascade (ligand unknown) (Bridges et al., 2020), and through the current work, polyamine signaling via NspS-MbaA. We propose that integrating the information contained in these different stimuli into the control of biofilm dispersal endows *V. cholerae* with the ability to successfully evaluate multiple features of its fluctuating environment prior to committing to the launch of this key lifestyle transition that, ultimately, impinges on its overall survival. Because *V. cholerae* biofilm formation and biofilm dispersal are intimately connected with cholera disease and its transmission, we suggest that deliberately controlling the biofilm lifecycle, possibly via synthetic strategies that target polyamine signal transduction via NspS-MbaA could be a viable therapeutic strategy to ameliorate disease.

Materials and Methods

Bacterial strains, reagents, and imaging assays

The *V. cholerae* strain used in this study was WT O1 El Tor biotype C6706str2. Antibiotics were used at the following concentrations: polymyxin B, 50 μ g/mL; kanamycin, 50 μ g/mL; spectinomycin, 200 μ g/mL; chloramphenicol, 1 μ g/mL; and gentamicin, 15 μ g/mL. Strains were propagated for cloning purposes in lysogeny broth (LB) supplemented with 1.5% agar or in liquid LB with shaking at 30°C. For biofilm dispersal analyses, *lux* measurements, c-di-GMP reporter quantitation, and norspermidine measurements, *V. cholerae* strains were grown in M9 medium supplemented with 0.5% dextrose and 0.5% casamino acids. All strains used in this work are reported in the Key Resources Table. Compounds were added from the onset of biofilm initiation. Norspermidine (Millipore Sigma, I1006-100G-A) and spermidine (Millipore Sigma, S2626-1G) were added at the final concentrations designated in the figures. The biofilm lifecycle was measured using time-lapse microscopy as described previously (Bridges and Bassler, 2019). All plots were generated using ggplot2 in R. Light production driven by the *vpsL* promoter was monitored as described previously (Bridges et al., 2020). Results from replicates were averaged and plotted using ggplot2 in R.

DNA manipulation and strain construction

All strains generated in this work were constructed by replacing genomic DNA with DNA introduced by natural transformation as previously described (Bridges et al., 2020). PCR and Sanger sequencing were used to verify correct integration events. Genomic DNA from recombinant strains was used for future co-transformations and as templates for PCR to generate DNA fragments, when necessary. See Key Resources Table for primers and g-blocks (IDT) used in this study. Gene deletions were constructed in frame and eliminated the entire coding sequences. The exceptions were *mbaA* and *nspS*, which overlap with adjacent genes, so an internal portion of each gene was deleted, ensuring that adjacent genes were not perturbed. To construct *mbaA-3xFLAG* at the native *mbaA* locus, gene synthesis was used to preserve the coding sequence of the downstream gene. To achieve this, the overlapping region was duplicated. In the duplication, the start codon of the downstream gene was disabled by mutation. The coding sequencing of *mbaA* was preserved. The DNA specifying *3xFLAG* was introduced immediately upstream of the *mbaA* stop codon. All strains constructed in this study were verified using the Genewiz sequencing service.

Western blotting

Cultures of strains carrying MbaA-3xFLAG and relevant catalytic site variants were collected at OD_{600} = 1.0 and subjected to centrifugation for 1 min at 13,000 rpm. The pellets were flash frozen, thawed for 5 min at 25° C, and subsequently chemically lysed by resuspending to OD_{600} = 1.0 in 75 µL Bug Buster (Novagen, #70584–4) supplemented with 0.5% Triton-X, 50 µg/mL lysozyme, 25 U/mL benzonase nuclease, and 1 mM phenylmethylsulfonyl fluoride (PMSF) for 10 min at 25° C. Lysates were solubilized in 1X SDS-PAGE buffer for 1 h at 37° C. Samples were loaded into 4–20% Mini-Protein TGX gels (Bio-Rad). Electrophoresis was carried out at 200 V. Proteins were transferred from the gels to PVDF membranes (Bio-Rad) for 50 min at 4° C at 100 V in 25 mM Tris base, 190 mM glycine, 20% methanol. Following transfer, membranes were blocked in 5% milk in PBST (137 mM NaCl, 2.7 mM KCl, 8 mM Na₂HPO₄, 2 mM KH₂PO₄, and 0.1% Tween) for 1 h, followed by three washes with PBST. Subsequently, membranes were

incubated for 1 h with a monoclonal Anti-FLAG-Peroxidase antibody (Millipore Sigma, #A8592) at a 1:5,000 dilution in PBST with 5% milk. After washing six times with PBST for 5 min each, membranes were exposed using the Amersham ECL Western blotting detection reagent (GE Healthcare). For the RpoA loading control, the same protocol was followed except that the primary antibody was Anti-Escherichia coli RNA Polymerase α (Biolegend, #663104) used at a 1:10,000 dilution and the secondary antibody was an Anti-Mouse IgG HRP conjugated antibody (Promega, #W4021) used at a 1:10,000 dilution.

Extraction and measurements of polyamines

To measure intracellular polyamines, previously established techniques were followed with slight modifications (McGinnis et al., 2009). For planktonic cell measurements, V. cholerae strains were grown in 5 mL of M9 medium containing glucose and casamino acids with constant shaking at 30° C. 2.0 OD₆₀₀ equivalents of V. cholerae cells were collected by centrifugation for 1 min at 13,000 rpm from cultures that had been grown to OD₆₀₀ ~2.0. Cells were washed once with 1x PBS and subsequently weighed and resuspended in 100 µL PBS. The resuspended cells were lysed by 10 freeze-thaw cycles in liquid nitrogen. After the final freeze-thaw cycle, samples were subjected to bath sonication for 20 s (Fisher Scientific, FS30) and subsequently diluted to 100 mg/mL in 1x PBS. To precipitate proteins, 100 μL of 50% trichloroacetic acid was added to 500 µL of lysate and the mixtures were incubated for 5 min. Precipitated material was pelleted by centrifugation for 5 min at 13,000 rpm. 500 µL of the resulting clarified supernatants were subjected to benzoylation as described below. For measurements of polyamines in cell-free culture fluids, the culture fluids from the samples described above were collected following the centrifugation step. Remaining cells were removed by filtration with 0.45 µm filters (Millex-HV), proteins were precipitated as above, and the benzoylation derivatization was performed. For measurements of polyamine concentrations in static cultures at the 5 h and 10 h timepoints, the procedure was the same as above with the following modifications: 10 mL cultures were incubated at 30° C without shaking to achieve conditions favoring the biofilm lifecycle. In the case of the 5 h cultures, samples were briefly mixed by vortex with sterile 1 mm glass beads to dislodge biofilms prior to centrifugation. Cell pellets from both the 5 h and 10 h samples were resuspended in 1x PBS at 40 mg/mL, proteins were precipitated, and 500 µL was used for derivatization.

Samples were derivatized with benzoyl chloride as previously described, except that the amount of benzoyl chloride was doubled to ~80 μ mol, and benzylated polyamines were resuspended in 200 μ L of the mobile phase (Morgan, 1998). In all cases, medium blanks and polyamine standards were simultaneously derivatized and analyzed to generate calibration curves. HPLC was performed on a Shimadzu UFLC system with PAL autoinjector. Thirty mingradient chromatography separation was performed using solvent A (10% methanol / 90% water) and solvent B (95% methanol / 5% water) on an ACE Ultracore 2.5 SuperC18 1.0 x 50 mm column with 63 μ L/min flow rate at a column temperature of 54° C. Mass spectrometry was performed using an Orbitrap XL mass spectrometer (Thermo) with an APCI ionization source in positive mode. The parent ion (MS1) was detected in the Orbitrap with 100,000 mass resolution and fragment ions (MS2) were detected in the ion trap. Parameters were as follows: the vaporizer temperature was 270° C, the sheath gas flow rate was 18 a.u., the auxiliary gas flow rate was 5 a.u., the sweep gas flow rate was 5 a.u., the discharge current was 9 mA, the capillary temperature was 250° C, the capillary voltage was 36 V, and the tube lens was 72 V. Skyline software (University of Washington) was used to analyze results.

c-di-GMP reporter assays

The c-di-GMP reporter has been described (Zamorano-Sánchez et al., 2019; Zhou et al., 2016). To measure relative reporter output for each condition, 100 μ L of *V. cholerae* cultures were back diluted to OD₆₀₀ = 0.0002 following overnight growth. Cultures were dispensed into 96-well plates containing the indicated polyamines and the plates were covered in breathe-easy membranes to prevent evaporation. Samples were incubated overnight at 30° C with shaking. The following morning, the breathe-easy membranes were removed and fluorescence measurements were obtained using a BioTek Synergy Neo2 Multi-Mode reader. For AmCyan, the excitation wavelength was 440±20 nm and emission was detected at 490±20 nm and for TurboRFP, the excitation wavelength was 530±20 nm and the emission was 575±20 nm. The c-di-GMP-regulated TurboRFP fluorescence was divided by the constitutive AmCyan fluorescence to yield the relative fluorescence intensity (RFI). To facilitate comparisons between strains and conditions, RFIs were subsequently normalized to the untreated *V. cholerae* WT RFI and the data are expressed as the percentage differences (denoted relative reporter signal). All results were obtained in biological triplicate and data analysis and plotting were performed in R.

Acknowledgements

We thank members of the Bassler group and Prof. Ned Wingreen for thoughtful discussions. The c-di-GMP reporter plasmid was a gift from Fitnat Yildiz (UC Santa Cruz). Mass spectrometry was conducted by the Princeton Molecular Biology Proteomics and Mass Spectrometry Core Facility. This work was supported by the Howard Hughes Medical Institute, NIH Grant 5R37GM065859, National Science Foundation Grant MCB-1713731, and a Max Planck-Alexander von Humboldt research award to BLB. AAB is a Howard Hughes Medical Institute Fellow of the Damon Runyon Cancer Research Foundation, DRG-2302-17. The content is solely the responsibility of the authors and does not necessarily represent the official views of the National Institutes of Health. The funders had no role in study design, data collection and analysis, decision to publish, or preparation of the manuscript.

Conflict of Interest

The authors declare no conflict of interest.

Figure 2 - figure supplement 1

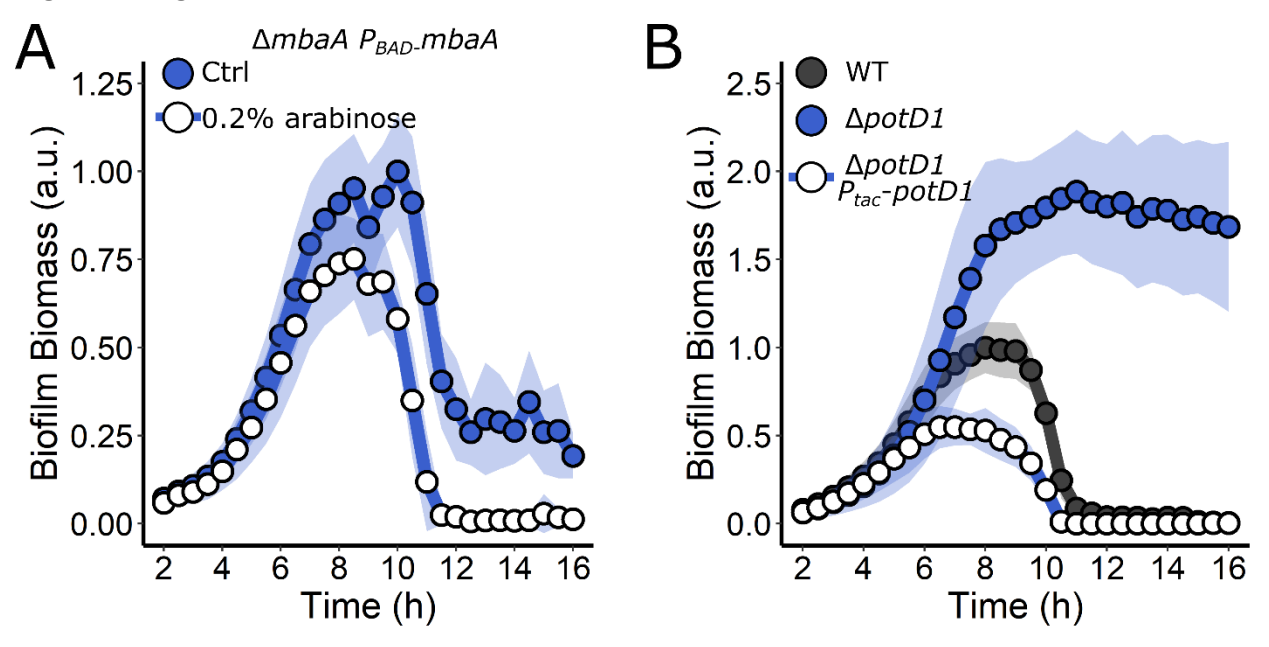


Figure 2 - figure supplement 1. *mbaA* and *potD1* complement the Δ *mbaA* and Δ *potD1* mutants, respectively. (A) Quantitation of biofilm biomass over time measured by time-lapse microscopy for the Δ *mbaA* P_{BAD} -*mbaA* strain following addition of water (Ctrl) or 0.2% arabinose. (B) Quantitation of biofilm biomass over time measured by time-lapse microscopy for the WT, Δ *potD1*, and Δ *potD1* strains. Data are represented as means normalized to the peak biofilm biomass of the Ctrl (left panel) or WT strain (right panel). N = 3 biological and N = 3 technical replicates, \pm SD (shaded). a.u., arbitrary unit.

Figure 2 - figure supplement 2

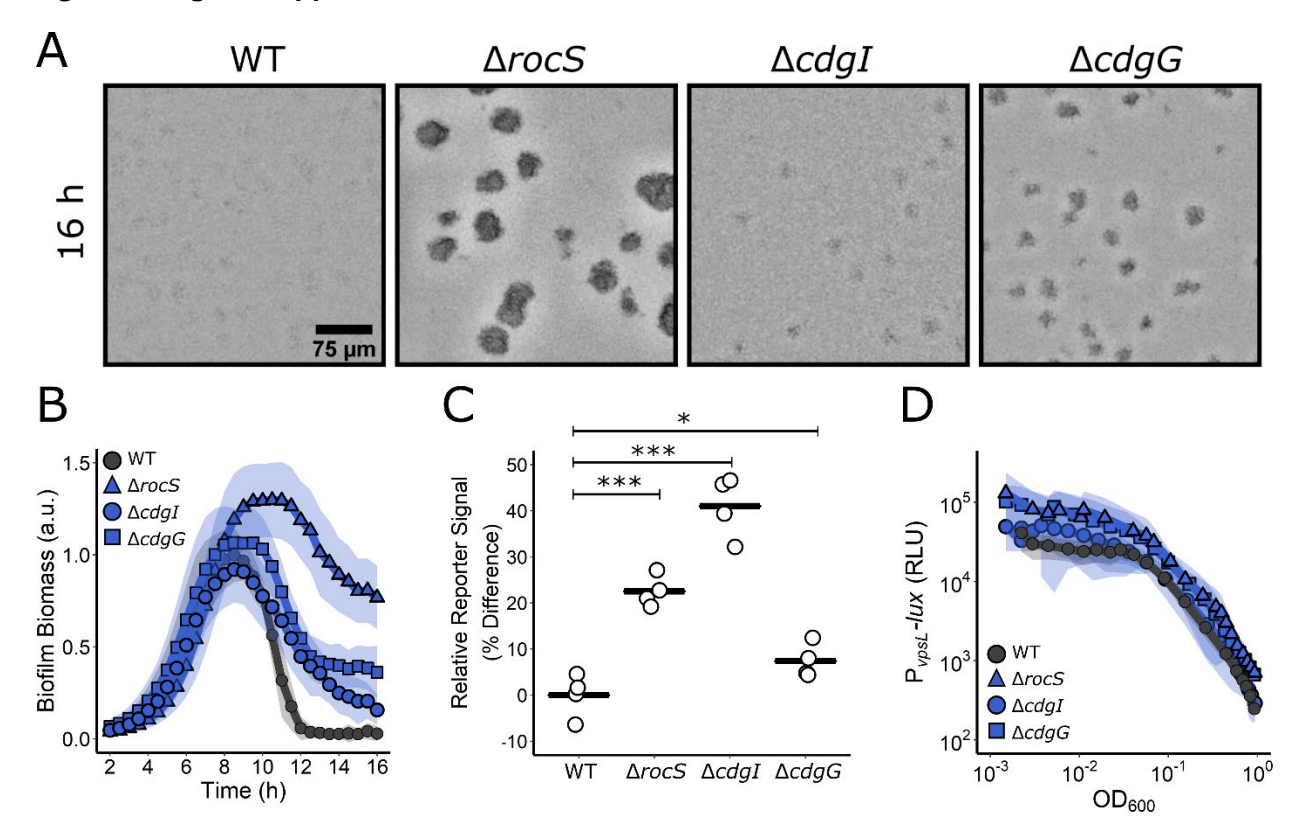


Figure 2 - figure supplement 2. **C-di-GMP signaling controls biofilm dispersal.** (A) Representative brightfield images of biofilms at 16 h for the designated strains. (B) Quantitation of biofilm biomass over time measured by time-lapse microscopy for WT and the designated mutants. Data are represented as means normalized to the peak biofilm biomass of the WT strain. N = 3 biological and N = 3 technical replicates, \pm SD (shaded). a.u., arbitrary unit. (C) Relative c-di-GMP reporter signals for the indicated strains. Values are expressed as the percentage difference relative to the WT strain. N = 4 biological replicates. Each black bar shows the sample mean. Unpaired t-tests were performed for statistical analysis, with P values denoted as *P < 0.05; *** P < 0.001. (D) The corresponding *PvpsL-lux* reporter output for the strains and growth conditions in B over the growth curve. RLU, relative light units. N = 3 biological replicates, \pm SD (shaded).

Figure 3 - figure supplement 1

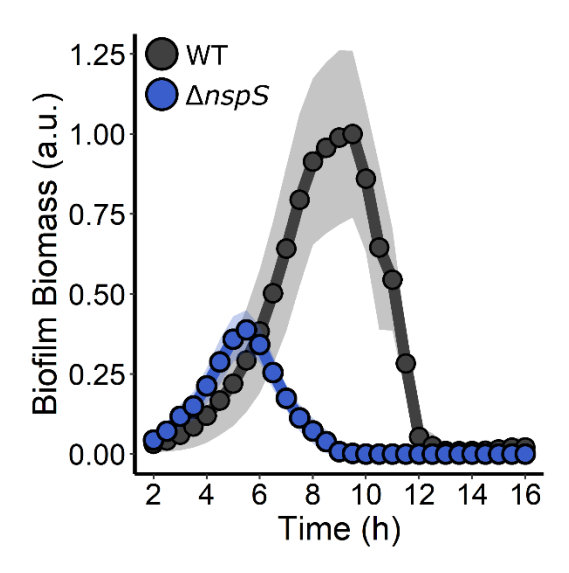


Figure 3 - figure supplement 1. **NspS is required for** *V. cholerae* **biofilm formation.** Quantitation of biofilm biomass over time measured by time-lapse microscopy for WT *V. cholerae* and the $\Delta nspS$ strain. For each strain, N=3 biological and N=3 technical replicates, \pm SD (shaded). a.u., arbitrary unit.

Figure 4 - figure supplement 1

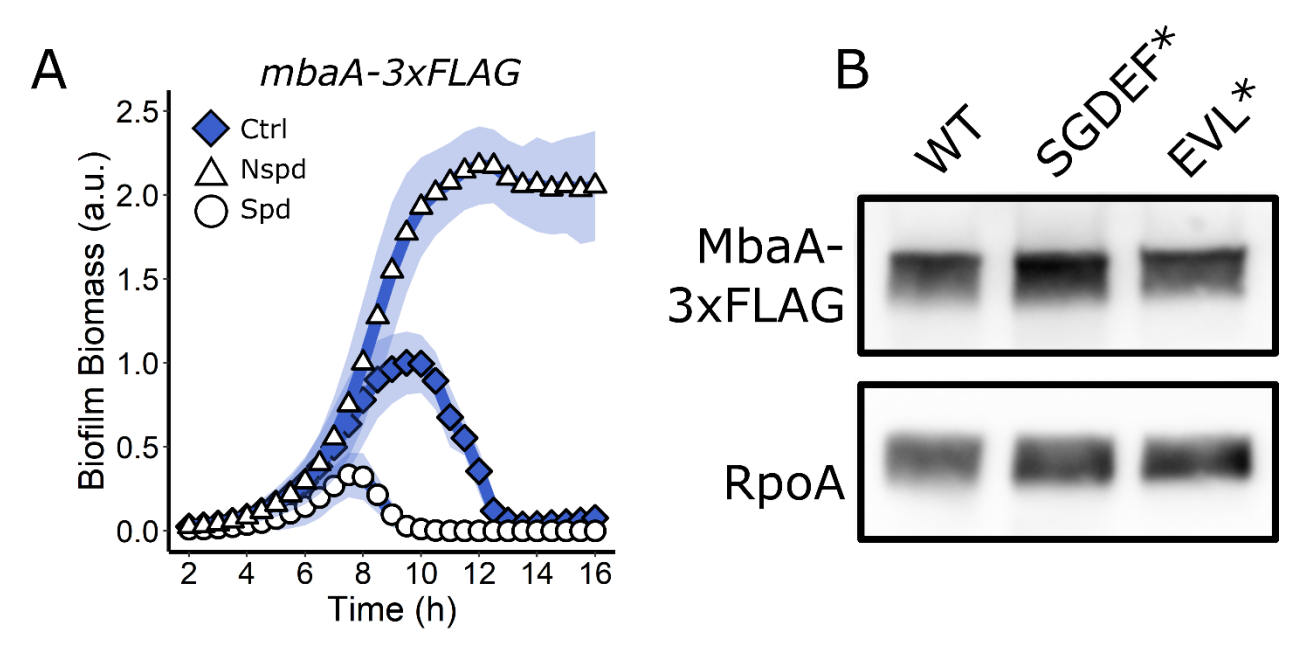


Figure 4 - figure supplement 1. **MbaA active site mutations do not alter protein levels.** (A) Quantitation of biofilm biomass over time measured by time-lapse microscopy for *V. cholerae* carrying MbaA-3xFLAG following addition of a water (Ctrl), 100 μ M norspermidine, or 100 μ M spermidine. Biofilm biomass data are represented as means normalized to the peak biofilm biomass of the WT strain or Ctrl condition. In all cases, N=3 biological and N=3 technical replicates, \pm SD (shaded). a.u., arbitrary unit. (B) Top panel: Western blot showing 3xFLAG for the WT MbaA, MbaA SGDEF*, and MbaA EVL* proteins. Bottom panel: RpoA is the loading control. Data are representative of three biological replicates.

Figure 5 - figure supplement 1

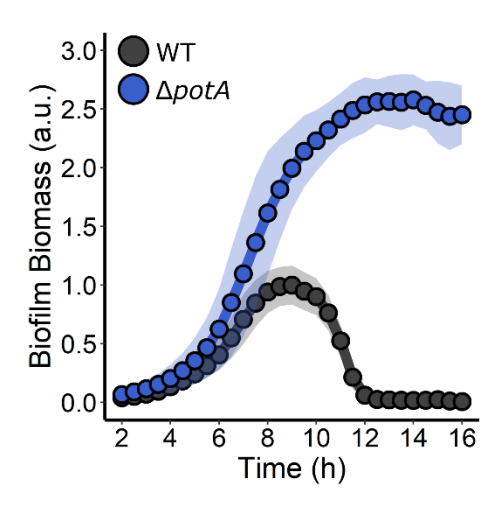
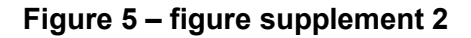


Figure 5 - figure supplement 1. **PotA is required for** *V. cholerae* **biofilm dispersal.** Quantitation of biofilm biomass over time measured by time-lapse microscopy for WT *V. cholerae* and the $\Delta potA$ strain. For each strain, N = 3 biological and N = 3 technical replicates, \pm SD (shaded). a.u., arbitrary unit.



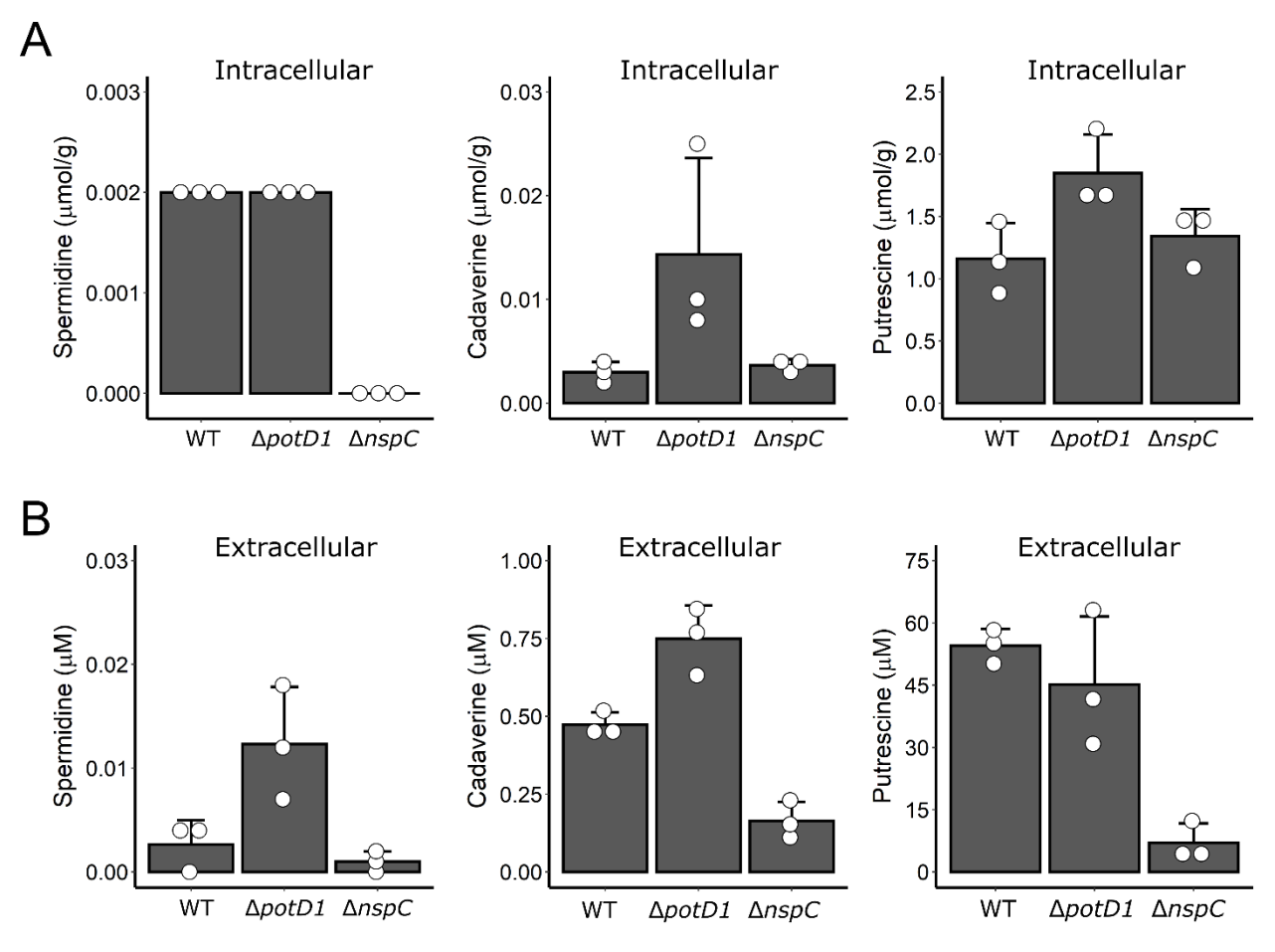


Figure 5 – figure supplement 2. **Polyamine levels for WT**, Δ *potD1*, and Δ *nspC* strains. (A) Intracellular spermidine (left panel), cadaverine (middle panel), and putrescine (right panel) levels normalized to wet cell pellet mass for the samples from Fig. 5 I, J. (B) Molar concentrations of polyamines in the cell-free culture fluids of the strains from panel A. The strains used in panels I and J also contained a Δ *vpsL* mutation to abolish biofilm formation. Thus, all strains existed in the same growth state which enabled comparisons between strains and, moreover, eliminated any possibility of polyamine sequestration by the biofilm matrix. N = 3 biological replicates. Error bars represent SDs.

Figure 6 - figure supplement 1

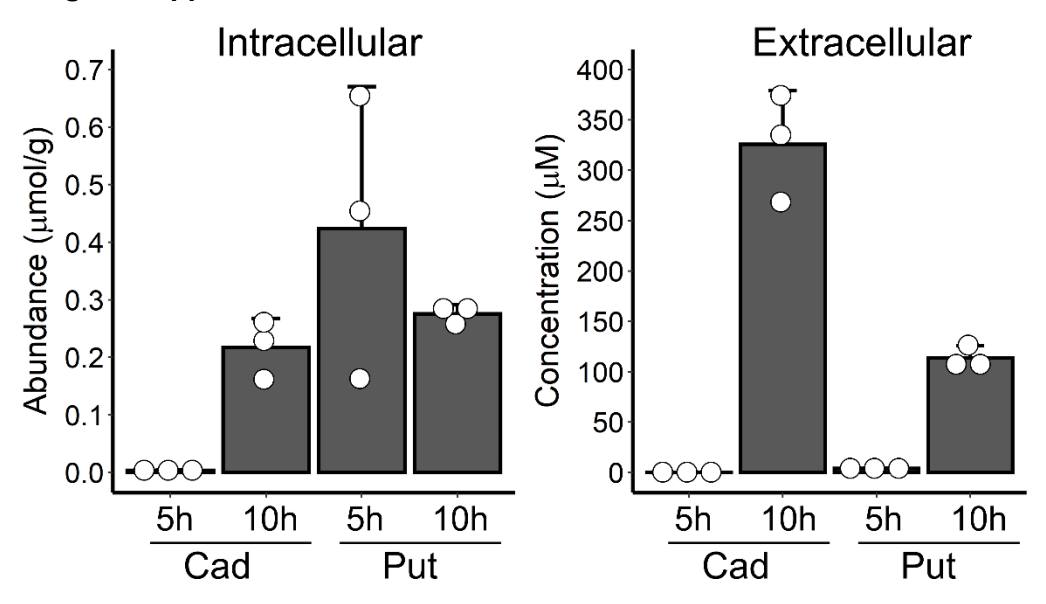


Figure 6 – figure supplement 1. Polyamine levels in WT V. cholerae prior to and following biofilm dispersal. Measurements of intracellular (left panel) and extracellular (right panel) cadaverine (Cad) and putrescine (Put) levels at 5 h and 10 h post inoculation for the samples shown in Fig. 6B. Intracellular levels were normalized to wet cell pellet mass. N = 3 biological samples. Error bars represent SDs.

Data availability

All data generated and analyzed in this study are included in the manuscript and supporting files. Source data files have been provided in Zenodo (https://doi.org/10.5281/zenodo.4651348).

Supplementary File 1. (separate file). C-di-GMP reporter output averages and standard deviations.

Video 1 (separate file). Representative time-lapse images of the biofilm lifecycles of the WT, $\Delta mbaA$, $\Delta potD1$, and $\Delta mbaA$ $\Delta potD1$ *V. cholerae* strains following treatment with water (Ctrl), 100 μM norspermidine (Nspd), or 100 μM spermidine (Spd).

Video 2 (separate file). Representative time-lapse images of the biofilm lifecycles of the *mbaA-3xFLAG*, *mbaA^{EVL*}-3xFLAG*, and *mbaA^{SGDEF*}-3xFLAG V. cholerae* strains following treatment with water (Ctrl), 100 μM norspermidine (Nspd), or 100 μM spermidine (Spd).

References

- Bassler BL, Wright M, Silverman MR. 1994. Multiple signaling systems controlling expression of luminescence in *Vibrio harveyi*: sequence and function of genes encoding a second sensory pathway. *Mol Microbiol* **13**:273–286. doi:10.1111/j.1365-2958.1994.tb00422.x
- Benamouzig R, Mahé S, Luengo C, Rautureau J, Tomé D. 1997. Fasting and postprandial polyamine concentrations in the human digestive lumen. *Am J Clin Nutr* **65**:766–770. doi:10.1093/ajcn/65.3.766
- Bomchil N, Watnick P, Kolter R. 2003. Identification and characterization of a *Vibrio cholerae* gene, MbaA, involved in maintenance of biofilm architecture. *J Bacteriol* **185**:1384–1390. doi:10.1128/JB.185.4.1384-1390.2003
- Boyd CD, Chatterjee D, Sondermann H, O'Toole GA. 2012. LapG, required for modulating biofilm formation by *Pseudomonas fluorescens* Pf0-1, is a calcium-dependent protease. *J Bacteriol* **194**:4406–4414. doi:10.1128/JB.00642-12
- Bridges AA, Bassler BL. 2019. The intragenus and interspecies quorum-sensing autoinducers exert distinct control over *Vibrio cholerae* biofilm formation and dispersal. *PLoS Biol* **17**:e3000429. doi:10.1371/journal.pbio.3000429
- Bridges AA, Fei C, Bassler BL. 2020. Identification of signaling pathways, matrix-digestion enzymes, and motility components controlling Vibrio cholerae biofilm dispersal. *Proc Natl Acad Sci USA* **117** (51) 32639-32647. https://doi.org/10.1073/pnas.2021166117
- Christen M, Christen B, Folcher M, Schauerte A, Jenal U. 2005. Identification and characterization of a cyclic di-GMP-specific phosphodiesterase and its allosteric control by GTP. *J Biol Chem* **280**:30829–30837. doi:10.1074/jbc.M504429200
- Christensen DG, Marsden AE, Hodge-Hanson K, Essock-Burns T, Visick KL. 2020. LapG mediates biofilm dispersal in *Vibrio fischeri* by controlling maintenance of the VCBS-containing adhesin LapV. *Mol Microbiol* **114**:742–761. doi:10.1111/mmi.14573
- Cockerell SR, Rutkovsky AC, Zayner JP, Cooper RE, Porter LR, Pendergraft SS, Parker ZM, McGinnis MW, Karatan E. 2014. *Vibrio cholerae* NspS, a homologue of ABC-type periplasmic solute binding proteins, facilitates transduction of polyamine signals independent of their transport. *Microbiology* **160**:832–843. doi:10.1099/mic.0.075903-0
- Conner JG, Teschler JK, Jones CJ, Yildiz FH. 2016. Staying alive: *Vibrio cholerae*'s cycle of environmental survival, transmission, and dissemination. *Microbiol Spectr* **4**. doi:10.1128/microbiolspec.VMBF-0015-2015
- Conner JG, Zamorano-Sánchez D, Park JH, Sondermann H, Yildiz FH. 2017. The ins and outs of cyclic di-GMP signaling in *Vibrio cholerae*. *Curr Opin Microbiol* **36**:20–29. doi:10.1016/j.mib.2017.01.002
- Flemming H-C, Wingender J, Szewzyk U, Steinberg P, Rice SA, Kjelleberg S. 2016. Biofilms: an emergent form of bacterial life. *Nat Rev Microbiology* **14**:563–575. doi:10.1038/nrmicro.2016.94
- Gallego-Hernandez AL, DePas WH, Park JH, Teschler JK, Hartmann R, Jeckel H, Drescher K, Beyhan S, Newman DK, Yildiz FH. 2020. Upregulation of virulence genes promotes *Vibrio cholerae* biofilm hyperinfectivity. *Proc Natl Acad Sci USA* **117**:11010–11017. doi:10.1073/pnas.1916571117
- Gjermansen M, Ragas P, Sternberg C, Molin S, Tolker-Nielsen T. 2005. Characterization of starvation-induced dispersion in *Pseudomonas putida* biofilms. *Environ Microbiol* **7**:894–904. doi:https://doi.org/10.1111/j.1462-2920.2005.00775.x
- Guilhen C, Forestier C, Balestrino D. 2017. Biofilm dispersal: multiple elaborate strategies for dissemination of bacteria with unique properties. *Mol Microbiol* **105**:188–210. doi:10.1111/mmi.13698

- Hamana K. 1997. Polyamine distribution patterns within the families Aeromonadaceae, Vibrionaceae, Pasteurellaceae, and Halomonadaceae, and related genera of the gamma subclass of the Proteobacteria. *J Gen Appl Microbiol* **43**:49–59. doi:10.2323/jgam.43.49
- Hobley L, Kim SH, Maezato Y, Wyllie S, Fairlamb AH, Stanley-Wall NR, Michael AJ. 2014. Norspermidine is not a self-produced trigger for biofilm disassembly. *Cell* **156**:844–854. doi:10.1016/j.cell.2014.01.012
- Joelsson A, Liu Z, Zhu J. 2006. Genetic and phenotypic diversity of quorum-sensing systems in clinical and environmental isolates of *Vibrio cholerae*. *Infect Immun* **74**:1141–1147. doi:10.1128/IAI.74.2.1141-1147.2006
- Karatan E, Duncan TR, Watnick PI. 2005. NspS, a predicted polyamine sensor, mediates activation of *Vibrio cholerae* biofilm formation by norspermidine. *J Bacteriol* **187**:7434–7443. doi:10.1128/JB.187.21.7434-7443.2005
- Karatan E, Michael AJ. 2013. A wider role for polyamines in biofilm formation. *Biotechnol Lett* **35**:1715–1717. doi:10.1007/s10529-013-1286-3
- Kashiwagi K, Innami A, Zenda R, Tomitori H, Igarashi K. 2002. The ATPase activity and the functional domain of PotA, a component of the sermidine-preferential uptake system in *Escherichia coli. J Biol Chem* **277**:24212–24219. doi:10.1074/jbc.M202849200
- Ke X, Miller LC, Bassler BL. 2015. Determinants governing ligand specificity of the *Vibrio harveyi* LuxN quorum-sensing receptor. *Mol Microbiol* **95**:127–142. doi:10.1111/mmi.12852
- Kitts G, Giglio KM, Zamorano-Sánchez D, Park JH, Townsley L, Cooley RB, Wucher BR, Klose KE, Nadell CD, Yildiz FH, Sondermann H. 2019. A conserved regulatory circuit controls large adhesins in *Vibrio cholerae. mBio* **10**. doi:10.1128/mBio.02822-19
- Lee J, Sperandio V, Frantz DE, Longgood J, Camilli A, Phillips MA, Michael AJ. 2009. An alternative polyamine biosynthetic pathway is widespread in bacteria and essential for biofilm formation in *Vibrio cholerae*. *J Biol Chem* **284**:9899–9907. doi:10.1074/jbc.M900110200
- McEvoy FA, Hartley CB. 1975. Polyamines in cystic fibrosis. *Pediatr Res* **9**:721–724. doi:10.1203/00006450-197509000-00007
- McGinnis MW, Parker ZM, Walter NE, Rutkovsky AC, Cartaya-Marin C, Karatan E. 2009. Spermidine regulates *Vibrio cholerae* biofilm formation via transport and signaling pathways. *FEMS Microbiol Lett* **299**:166–174. doi:10.1111/j.1574-6968.2009.01744.x
- Michael AJ. 2018. Polyamine function in archaea and bacteria. *J Biol Chem* **293**:18693–18701. doi:10.1074/jbc.TM118.005670
- Miller-Fleming L, Olin-Sandoval V, Campbell K, Ralser M. 2015. Remaining mysteries of molecular biology: the role of polyamines in the cell. *J Mol Biol*, OMICS Approaches to Unravel Molecular Function, Part II **427**:3389–3406. doi:10.1016/j.jmb.2015.06.020
- Morgan DML. 1998. Determination of polyamines as their benzoylated derivatives by HPLC In: Morgan DML, editor. Polyamine Protocols, Methods in Molecular Biology™. Totowa, NJ: Humana Press. pp. 111–118. doi:10.1385/0-89603-448-8:111
- Nesse LL, Berg K, Vestby LK. 2015. Effects of norspermidine and spermidine on biofilm formation by potentially pathogenic *Escherichia coli* and *Salmonella enterica* wild-type strains. *Appl Environ Microbiol* 81:2226–2232. doi:10.1128/AEM.03518-14
- Newell PD, Boyd CD, Sondermann H, O'Toole GA. 2011. A c-di-GMP effector system controls cell adhesion by inside-out signaling and surface protein cleavage. *PLOS Biol* **9**:e1000587. doi:10.1371/journal.pbio.1000587
- Osborne DL, Seidel ER. 1990. Gastrointestinal luminal polyamines: cellular accumulation and enterohepatic circulation. *Am J Physiol* **258**:G576-584. doi:10.1152/ajpqi.1990.258.4.G576
- Papenfort K, Bassler BL. 2016. Quorum sensing signal-response systems in Gram-negative bacteria. *Nat Rev Microbiol* **14**:576–588. doi:10.1038/nrmicro.2016.89

- Parker ZM, Pendergraft SS, Sobieraj J, McGinnis MM, Karatan E. 2012. Elevated levels of the norspermidine synthesis enzyme NspC enhance *Vibrio cholerae* biofilm formation without affecting intracellular norspermidine concentrations. *FEMS Microbiol Lett* **329**:18–27. doi:10.1111/j.1574-6968.2012.02498.x
- Patel CN, Wortham BW, Lines JL, Fetherston JD, Perry RD, Oliveira MA. 2006. Polyamines are essential for the formation of plague biofilm. *J Bacteriol* **188**:2355–2363. doi:10.1128/JB.188.7.2355-2363.2006
- Pérez-Mendoza D, Coulthurst SJ, Humphris S, Campbell E, Welch M, Toth IK, Salmond GPC. 2011. A multi-repeat adhesin of the phytopathogen, *Pectobacterium atrosepticum*, is secreted by a Type I pathway and is subject to complex regulation involving a non-canonical diguanylate cyclase. *Mol Microbiol* 82:719–733. doi:10.1111/j.1365-2958.2011.07849.x
- Puleston DJ, Buck MD, Klein Geltink RI, Kyle RL, Caputa G, O'Sullivan D, Cameron AM, Castoldi A, Musa Y, Kabat AM, Zhang Y, Flachsmann LJ, Field CS, Patterson AE, Scherer S, Alfei F, Baixauli F, Austin SK, Kelly B, Matsushita M, Curtis JD, Grzes KM, Villa M, Corrado M, Sanin DE, Qiu J, Pällman N, Paz K, Maccari ME, Blazar BR, Mittler G, Buescher JM, Zehn D, Rospert S, Pearce EJ, Balabanov S, Pearce EL. 2019. Polyamines and eIF5A hypusination modulate mitochondrial respiration and macrophage activation. *Cell Metab* 30:352-363.e8. doi:10.1016/j.cmet.2019.05.003
- Römling U, Galperin MY, Gomelsky M. 2013. Cyclic di-GMP: the first 25 years of a universal bacterial second messenger. *Microbiol Mol Biol Rev* **77**:1–52. doi:10.1128/MMBR.00043-12
- Singh PK, Bartalomej S, Hartmann R, Jeckel H, Vidakovic L, Nadell CD, Drescher K. 2017. *Vibrio cholerae* combines individual and collective sensing to trigger biofilm dispersal. *Current Biology* **27**:3359-3366.e7. doi:10.1016/j.cub.2017.09.041
- Sobe RC, Bond WG, Wotanis CK, Zayner JP, Burriss MA, Fernandez N, Bruger EL, Waters CM, Neufeld HS, Karatan E. 2017. Spermine inhibits *Vibrio cholerae* biofilm formation through the NspS–MbaA polyamine signaling system. *J Biol Chem* **292**:17025–17036. doi:10.1074/jbc.M117.801068
- Tamayo R, Patimalla B, Camilli A. 2010. Growth in a biofilm induces a hyperinfectious phenotype in *Vibrio cholerae*. *Infection and Immunity* **78**:3560–3569. doi:10.1128/IAI.00048-10
- Wotanis CK, Iii WPB, Angotti AD, Villa EA, Zayner JP, Mozina AN, Rutkovsky AC, Sobe RC, Bond WG, Karatan E. 2017. Relative contributions of norspermidine synthesis and signaling pathways to the regulation of *Vibrio cholerae* biofilm formation. *PLOS ONE* **12**:e0186291. doi:10.1371/journal.pone.0186291
- Yamamoto S, Chowdhury MA, Kuroda M, Nakano T, Koumoto Y, Shinoda S. 1991. Further study on polyamine compositions in Vibrionaceae. *Can J Microbiol* **37**:148–153. doi:10.1139/m91-022
- Young EC, Baumgartner JT, Karatan E, Kuhn ML. 2021. A mutagenic screen reveals NspS residues important for regulation of *Vibrio cholerae* biofilm formation. *Microbiology* doi:10.1099/mic.0.001023
- Zamorano-Sánchez D, Xian W, Lee CK, Salinas M, Thongsomboon W, Cegelski L, Wong GCL, Yildiz FH. 2019. Functional specialization in *Vibrio cholerae* diguanylate cyclases: distinct modes of motility suppression and c-di-GMP production. *mBio* **10**. doi:10.1128/mBio.00670-19
- Zhou H, Zheng C, Su J, Chen B, Fu Y, Xie Y, Tang Q, Chou S-H, He J. 2016. Characterization of a natural triple-tandem c-di-GMP riboswitch and application of the riboswitch-based dual-fluorescence reporter. *Scientific Reports* **6**:20871. doi:10.1038/srep20871

Key Resources Table				
Reagent type (species) or resource	Designation	Source or reference	Identifiers	Additional information
strain, strain background (<i>Vibrio</i> <i>cholerae</i>)	BB_Vc_0090	Laboratory WT	WT O1 El Tor biotype C6706str2	-
strain, strain background (<i>Vibrio</i> <i>cholerae</i>)	AB_Vc_761	Bridges et al. 2020	Δ <i>vc1807</i> ::Cm ^R (Referred to as WT)	-
strain, strain background (<i>Vibrio</i> <i>cholerae</i>)	AB_Vc_839	Bridges et al. 2020	Δ <i>mbaA</i> Δ <i>vc1807</i> ::Kan ^R	-
strain, strain background (<i>Vibrio</i> <i>cholerae</i>)	AB_Vc_928	Natural transformation of BB_Vc_0090	Δ <i>nspS</i> Δ <i>vc1807</i> ::Kan ^R	-
strain, strain background (<i>Vibrio</i> <i>cholerae</i>)	AB_Vc_711	Bridges et al. 2020	Δ <i>potD1</i> Δ <i>vc1807</i> ::Cm ^R	-
strain, strain background (<i>Vibrio</i> <i>cholerae</i>)	AB_Vc_758	Bridges et al. 2020	ΔrocS Δvc1807::Cm ^R	-
strain, strain background (<i>Vibrio</i> <i>cholerae</i>)	AB_Vc_777	Bridges et al. 2020	Δ <i>cdgl</i> Δ <i>vc1807</i> ::Cm ^R	-
strain, strain background (<i>Vibrio</i> <i>cholerae</i>)	AB_Vc_778	Bridges et al. 2020	Δ <i>cdgG</i> Δ <i>vc1807</i> ::Cm ^R	-
strain, strain background (<i>Vibrio</i> <i>cholerae</i>)	AB_Vc_835	Natural transformation of BB_Vc_0090	mbaA-3xFLAG Δvc1807::Kan ^R	-
strain, strain background (<i>Vibrio</i> <i>cholerae</i>)	AB_Vc_870	Natural transformation of BB_Vc_0090	mbaA(D426A, E427A)-3xFLAG Δvc1807:: Kan ^R	-
strain, strain background (<i>Vibrio</i> <i>cholerae</i>)	AB_Vc_872	Natural transformation of BB_Vc_0090	mbaA(E553A)- 3xFLAG Δvc1807::Kan ^R	-
strain, strain background (<i>Vibrio</i> <i>cholerae</i>)	AB_Vc_798	Natural transformation of AB_Vc_709	ΔmbaA ΔpotD1 Δvc1807::Kan ^R	-
strain, strain background (<i>Vibrio</i> <i>cholerae</i>)	AB_Vc_956	Conj. of BB_Vc_0090	WT	Carrying plasmid pFY4357::Gm ^R
strain, strain background (<i>Vibrio</i> <i>cholerae</i>)	AB_Vc_977	Conj. of AB_Vc_928	Δ <i>nspS</i> Δ <i>vc1807</i> ::Kan ^R	Carrying plasmid pFY4357::Gm ^R

strain, strain background (<i>Vibrio</i> <i>cholerae</i>)	AB_Vc_971	Conj. of AB_Vc_870	mbaA(D426A, E427A)- 3xFLAG Δνc1807:: Kan ^R	Carrying plasmid pFY4357::Gm ^R
strain, strain background (<i>Vibrio</i> <i>cholerae</i>)	AB_Vc_973	Conj. of AB_Vc_872	mbaA(E553A)-3xFLAG Δvc1807::Kan ^R	Carrying plasmid pFY4357::Gm ^R
strain, strain background (<i>Vibrio</i> <i>cholerae</i>)	AB_Vc_969	Conj. of AB_Vc_711	Δ <i>potD1</i> Δ <i>vc1807</i> ::Cm ^R	Carrying plasmid pFY4357::Gm ^R
strain, strain background (<i>Vibrio</i> <i>cholerae</i>)	AB_Vc_987	Conj. of AB_Vc_758	ΔrocS Δvc1807::Cm ^R	Carrying plasmid pFY4357::Gm ^R
strain, strain background (<i>Vibrio</i> <i>cholerae</i>)	AB_Vc_989	Conj. of AB_Vc_777	Δcdgl Δvc1807::Cm ^R	Carrying plasmid pFY4357::Gm ^R
strain, strain background (<i>Vibrio</i> <i>cholerae</i>)	AB_Vc_991	Conj. of AB_Vc_778	ΔcdgG Δvc1807::Cm ^R	Carrying plasmid pFY4357::Gm ^R
strain, strain background (<i>Vibrio</i> cholerae)	AB_Vc_801	Bridges et al. 2020	Δ <i>vc1</i> 807::Kan ^R	Carrying plasmid pEVS143- <i>P_{vpsL}</i> - <i>lux</i> ::Cm ^R
strain, strain background (<i>Vibrio</i> <i>cholerae</i>)	AB_Vc_848	Conj. of AB_Vc_839	Δ <i>mbaA</i> Δ <i>vc1807</i> ::Kan ^R	Carrying plasmid pEVS143- <i>P_{vpsL}</i> - <i>lux</i> ::Cm ^R
strain, strain background (Vibrio cholerae)	AB_Vc_828	Conj. of AB_Vc_810	Δ <i>potD1</i> Δ <i>vc1807</i> ::Kan ^R	Carrying plasmid pEVS143-P _{vpsL} - lux::Cm ^R
strain, strain background (<i>Vibrio</i> <i>cholerae</i>)	AB_Vc_830	Conj. of AB_Vc_812	ΔrocS Δvc1807::Kan ^R	Carrying plasmid pEVS143- <i>P_{vpsL}</i> - <i>lux</i> ::Cm ^R
strain, strain background (Vibrio cholerae)	AB_Vc_831	Conj. of AB_Vc_813	Δ <i>cdgl Δvc1807</i> ::Kan ^R	Carrying plasmid pEVS143-P _{vpsL} - lux::Cm ^R
strain, strain background (Vibrio cholerae)	AB_Vc_832	Conj. of AB_Vc_814	ΔcdgG Δvc1807::Kan ^R	Carrying plasmid pEVS143- <i>P_{vpsL}</i> - <i>lux</i> ::Cm ^R
strain, strain background (<i>Vibrio</i> <i>cholerae</i>)	AB_Vc_979	Natural transformation of BB_Vc_0090	Δ <i>vpsL</i> ::Cm ^R	-
strain, strain background (<i>Vibrio</i> <i>cholerae</i>)	AB_Vc_981	Natural transformation of AB_Vc_810	Δ <i>vpsL</i> ::Cm ^R Δ <i>potD1</i> Δ <i>vc1807</i> ::Kan ^R	-

AB_Vc_983	Natural transformation of AB_Vc_823	Δ <i>vpsL</i> ::Cm ^R Δ <i>nspC</i> Δ <i>vc1807</i> ::Kan ^R	-
AB_Vc_1068	Natural transformation of BB_Vc_0090	Δ <i>potA</i> Δ <i>vc1807</i> ::Kan ^R	-
AB_Vc_823	Natural transformation of BB_Vc_0090	ΔnspC Δvc1807::Kan ^R	-
AB_Vc_993	Natural transformation of AB_Vc_711	Δ <i>nspC</i> Δ <i>potD1</i> Δ <i>vc1807</i> ::Kan ^R	-
AB_Vc_856	Natural transformation of AB_Vc_839	ΔmbaA Δvc1807::P _{BAD} - mbaA::Spec ^R	-
AB_Vc_1090	Natural transformation of AB_Vc_711	ΔpotD1 Δvc1807::P _{tac} - potD1::Kan ^R	-
nspS_3000up	This paper	PCR primers for cloning at <i>nspS</i> locus	GACTTTATCAGGCCT ACTCGCGTTATCCCT G
nspS_2700up	This paper	PCR primers for cloning at <i>nspS</i> locus	CTCTACAAAGCGGAA CGTGGTTAACCG
nspS_100up	This paper	PCR primers for cloning at <i>nspS</i> locus	CTACCCTAGTGAAAA CGTCAAACCCACTCA G
nspS_del2_B	This paper	PCR primers for nspS deletion	CTCGGTGCTCTACA GGGAGCAAAGCTTC GTTACAAAAATTGGT CACGATCC
nspS_del2_C	This paper	PCR primers for <i>nspS</i> deletion	GGATCGTGACCAATT TTTGTAACGAAGCTT TGCTCCCTGTAGAG CACCGAG
nspS_100down	This paper	PCR primers for cloning at <i>nspS</i> locus	GATGATGTCACTTTT GGCCAGCGTG
nspS_2700down	This paper	PCR primers for cloning at <i>nspS</i> locus	CCTAATGACATCACT GGCTAAGCCGAG
nspS_3000down	This paper	PCR primers for cloning at <i>nspS</i> locus	CGCGTGGTTCGAAT GAGCTCAAGTC
mbaA_3000up	This paper	PCR primers for cloning at <i>mbaA</i> locus	GCGCGCTAATCTGA ACTCAACCCATAAG
	AB_Vc_1068 AB_Vc_823 AB_Vc_993 AB_Vc_856 AB_Vc_1090 nspS_3000up nspS_2700up nspS_100up nspS_del2_B nspS_del2_C nspS_100down nspS_3000down	AB_Vc_983 AB_Vc_1068 AB_Vc_1068 AB_Vc_823 AB_Vc_823 AB_Vc_823 AB_Vc_0090 AB_Vc_993 AB_Vc_993 AB_Vc_993 AB_Vc_856 AB_Vc_856 AB_Vc_1090 AB_Vc_839 AB_Vc_1090 AB_Vc_1090 AB_Vc_1090 AB_Vc_711 AB_Vc_839 AB_Vc_1090 AB_Vc_711 AB_Vc_1090 AB_Vc_711 AB_Vc_1090 AB_Vc_111 AB_Vc_1090 AB_Vc_111 AB_Vc_1090 AB_Vc_111 AB_Vc_111 AB_Vc_1090 AB_Vc_111 AB_Vc_111	AB_Vc_993 transformation of AB_Vc_823 Δvc1807::Kan ^R AB_Vc_1068 Natural transformation of BB_Vc_0090 ΔpotA Δvc1807::Kan ^R AB_Vc_823 Natural transformation of BB_Vc_0090 ΔnspC Δvc1807::Kan ^R AB_Vc_993 Natural transformation of AB_Vc_1100 ΔnspC ΔpotD1 Δvc1807::Kan ^R AB_Vc_993 Natural transformation of AB_Vc_711 ΔmbaA Δvc1807::PaAD-mbaA::Spec ^R AB_Vc_856 Natural transformation of AB_Vc_839 ΔpotD1 Δvc1807::PaAD-mbaA::Spec ^R AB_Vc_1090 Natural transformation of AB_Vc_711 PCR primers for cloning at nspS locus nspS_3000up This paper PCR primers for cloning at nspS locus nspS_100up This paper PCR primers for nspS deletion nspS_del2_B This paper PCR primers for nspS deletion nspS_100down This paper PCR primers for cloning at nspS locus nspS_2700down This paper PCR primers for cloning at nspS locus nspS_3000down This paper PCR primers for cloning at nspS locus

sequence-based reagent	mbaA_2700up	This paper	PCR primers for cloning at <i>mbaA</i> locus	CGTTAGCATTCCACG CGGTCAGTTAG
sequence-based reagent	mbaA_2700down	This paper	PCR primers for cloning at <i>mbaA</i> locus	GATCTCATGACGCG CCTGACGGTATTTAA G
sequence-based reagent	mbaA_3000down	This paper	PCR primers for cloning at <i>mbaA</i> locus	CATCGTTCGCGATAG TGGGAAATTCAATAA AATG
sequence-based reagent	mbaA_100up	This paper	PCR primers for cloning at <i>mbaA</i> locus	GAAACCTGACATTGC CGCAATCAATGC
sequence-based reagent	mbaA_100down	This paper	PCR primers for cloning at <i>mbaA</i> locus	CCTGCTTCCAATCCG ACATAATACTCTGC
sequence-based reagent	mbaA_FLAG_Gblock	This paper	Generating mbaA- 3xFLAG	GGTTATCCAATGAGC CTAAGCGAGATCTCC CCATGGCTTCACGC CTCCAATCATAAAAA GAAGAGTTATTGCT TCACAGAACCCAGC CAAAGTGAATGCCGT GAAAACCTGTATTTT CAGGGACGGGATCC GAATTCGAGCTCCGT CGACAAGCTTGCGG CCGCACTCGAGGAC TACAAAGACCATGAC GGTGATTATAAAGAT CATGATATCGATTAC AAGGATGACGATGA CAAGTGA
sequence-based reagent	mbaA_SNAP/FLAG_R	This paper	PCR primers for cloning mbaA-3xFLAG*	GAAGCCATGGGGAG ATCTCGCTTAGGCTC
sequence-based reagent	mbaA_3xFLAG_F	This paper	PCR primers for cloning mbaA-3xFLAG*	GATATCGATTACAAG GATGACGATGACAA GTGATCTCCCCATG GCTTCATGCCTCCAA TC

sequence-based reagent	mbaA_SGDEF_mutR	This paper	PCR primers for mutagenizing <i>mbaA</i> SGDEF	GACGAGCAAAATAG CAAACGCAGCACCA GATAAACGGGCC
sequence-based reagent	mbaA_SGDEF_mutF	This paper	PCR primers for mutagenizing <i>mbaA</i> SGDEF	GGCCCGTTTATCTG GTGCTGCGTTTGCTA TTTTGCTCGTC
sequence-based reagent	mbaA_EAL_mutR	This paper	PCR primers for mutagenizing <i>mbaA</i> EAL	GATTGCCAGCGCAG CAATACTGCGAAGC CCACTAAGCG
sequence-based reagent	mbaA_EAL_mutF	This paper	PCR primers for mutagenizing <i>mbaA</i> EAL	CGCTTAGTGGGCTT CGCAGTATTGCTGC GCTGGCAATC
sequence-based reagent	potD1_3000up	This paper	PCR primers for cloning at <i>potD1</i> locus	CTGGAATCCGGTAT GTGTGTGATGGTTAG
sequence-based reagent	potD1_3000down	This paper	PCR primers for cloning at <i>potD1</i> locus	AGAGCGACTAGGTG TTATTGAACTTGGG
sequence-based reagent	potD1_100up	This paper	PCR primers for cloning at <i>potD1</i> locus	CTAAGAAAAGCATCA AATAGGCAGCCATTG
sequence-based reagent	potD1_100down	This paper	PCR primers for cloning at <i>potD1</i> locus	GATCTGGAAGAGATT AAGGCGCTCTC
sequence-based reagent	nspC_3000up	This paper	PCR primers for cloning at <i>nspC</i> locus	CTGAGCAAGTTAACC AAGAGTGGAAAAAAC AC
sequence-based reagent	nspC_2700up	This paper	PCR primers for cloning at <i>nspC</i> locus	GCCGTGTTTGAAGA GGTGAAAGCACCCT ATTC
sequence-based reagent	nspC_100up	This paper	PCR primers for cloning at <i>nspC</i> locus	GCTTACCTGTAACTC CAAGTAGTTTGGGTA TAAAC
sequence-based reagent	nspC_B	This paper	PCR primers for nspC deletion	CTTCGAGTCCAGACA AAATATGTACTCGTC ATGCTTGTGATGGCA AATATCTCGATAACA AGAATG
sequence-based reagent	nspC_C	This paper	PCR primers for <i>nspC</i> deletion	CATTCTTGTTATCGA GATATTTGCCATCAC AAGCATGACGAGTA CATATTTTGTCTGGA CTCGAAG

sequence-based reagent	nspC_100dwn	This paper	PCR primers for cloning at <i>nspC</i> locus	CGACACTTCCTATGT AATCACTATCTTCAC AC
sequence-based reagent	nspC_2700dwn	This paper	PCR primers for cloning at <i>nspC</i> locus	CTTCGAAGCCGGAT GTATCAAATTGTGTT G
sequence-based reagent	nspC_2700dwn	This paper	PCR primers for cloning at <i>nspC</i> locus	GTAATTGGAGCCGTA GGAGCTTGCAG
sequence-based reagent	potA_3000up	This paper	PCR primers for cloning at <i>potA</i> locus	CGATCATTCCATGTA ACTTGTGTGGGTC
sequence-based reagent	potA_2700up	This paper	PCR primers for cloning at <i>potA</i> locus	GCAAGTCGTGGAAG ATGAAGACTTAGTG
sequence-based reagent	potA_B	This paper	PCR primers for cloning at <i>potA</i> locus	GCATTTTGTAGATTA AGCTTTTTGCTCATC ATCTCGGCCTGTAGA AAATCCTACTTGTTG
sequence-based reagent	potA_100down	This paper	PCR primers for cloning at <i>potA</i> locus	GGTGAATGCAAACTT AATCAGGTTCGC
sequence-based reagent	potA_2700down	This paper	PCR primers for cloning at <i>potA</i> locus	CAATGGCTGCCTATT TGATGCTTTTCTTAG
sequence-based reagent	potA_3000down	This paper	PCR primers for cloning at <i>potA</i> locus	GTAAAGTCTTCTAGG ACTTCGCTCGGG
sequence-based reagent	BBC1881	This paper	PCR primers for cloning at <i>vc1807</i> locus	TTTAAAGGGGATCAG TGACCG
sequence-based reagent	BBC1882	This paper	PCR primers for cloning at <i>vc1807</i> locus	CAATTTTGCTTTTGG ACCATCCC
sequence-based reagent	1807_2700up	This paper	PCR primers for cloning at <i>vc1807</i> locus	GGCCGGCACTTTGA TTACAATC
sequence-based reagent	1807_2700down	This paper	PCR primers for cloning at <i>vc1807</i> locus	GTCTATATCAGAGCG CTTAAAGAGCG
sequence-based reagent	PBAD_1807_Univ_B	This paper	PCR primers for generating PBAD-mbaA	CATTTCACACCTCCT GCAGGTAC
sequence-based reagent	Pbad-mbaA-1807_C	This paper	PCR primers for generating PBAD-mbaA	GTACCTGCAGGAGG TGTGAAATGAAGCTA

				AACCATAGAATTCTG TTACTGATTGCACC
sequence-based reagent	Pbad-mbaA-1807_D	This paper	PCR primers for generating PBAD-mbaA	GTCGACGGATCCCC GGAATCTAACGGCAT TCACTTTGGCTGGG
sequence-based reagent	Ptac_noRBS_R	This paper	PCR primers for generating Ptac-potD1	AATTGAATTCCTAGG CCTGTCGAGGCTG
sequence-based reagent	Ptac_potD1_RBS_C	This paper	PCR primers for generating Ptac-potD1	CAGCCTCGACAGGC CTAGGAATTCAATTA CGCCTAGTTAGGTTC TTTCTATACACTATG G
sequence-based reagent	Ptac-potD1-1807_D	This paper	PCR primers for generating <i>Ptac-potD1</i>	GTCGACGGATCCCC GGAATTTAATCGTTC ACTTTTAGCTTTTGG AAATACTCATCG
chemical compound, drug	Norspermidine	Millipore Sigma	I1006-100G-A	-
chemical compound, drug	Spermidine	Millipore Sigma	S2626-1G	-
antibody	Anti-FLAG-Peroxidase antibody	Millipore Sigma	#A8592	WB(1:5000)
antibody	Anti-Escherichia coli RNA Polymerase α	Biolegend	#663104	WB(1:10000)
antibody	Anti-Mouse IgG HRP conjugate	Promega	#W4021	WB(1:10000)
commercial assay or kit	Amersham ECL Western blotting detection reagent	GE Healthcare	45-000-875 /RPN2106	-
software, algorithm	FIJI		v. 1.53C	-
software, algorithm	RStudio		Version 1.4.1103	-